TÉCNICO LISBOA

Interpretation of the results of Static Load Tests on PLLN experimental piles

Miguel Ângelo Pedrosa Duarte

Thesis to obtain the Master of Science Degree in

Civil Engineering

Supervisor

Prof. Dr. Jaime Alberto dos Santos

Examination Committee

Chairperson: Prof. Drª. Teresa Maria Bodas de Araújo Freitas

Supervisor: Prof. Dr. Jaime Alberto dos Santos

Member of the Committee: Prof. Alexandre da Luz Pinto

Janeiro 2021

To my family

Declaration

I declare that this document is an original work of my own authorship and that it fulfils all the requirements of the Code of Conduct and Good Practices of the Universidade de Lisboa.

ACKONOWLEDGEMENTS

First of all, I would like to thank my supervisor Jaime Alberto dos Santos for guiding me during this work, for being patient during the discussion of the results and, most of all, by teaching me how to organize and how to be disciplined during the work - do not jump into conclusions, analyse the results first.

I would like to express my gratitude towards Mota-Engil S.A. for allowing me to explore the results of the biggest experimental field on piles, ever made on Iberian Peninsula.

I am so grateful to my parents and my brother. They were the key for never letting the interest disappear and to overcome all the problems that occurred. I have no words to describe the importance they had along this path. Just as all the problems were theirs, now, all my success are theirs too

A big thanks to Pedro and João for all the friendship and guidance along the path. They were crucial during the last times of this work and they did not let me down once, disregarding their own work to help me without demanding anything in return.

I am thankful to many friends that were always there along my academic years, but I cannot forget to mention Sónia, Duarte, Raquel, Ana Silva Karim, Ana Sousa, Ana Teresa, Cristiana, Juliana and Tiago that were important not only during the development of this work but also along my journey in Lisbon by making it feel like home.

Resumo

A análise de ensaios de carga estática têm-se revelados essenciais no estudo do comportamento de estacas e são vários os autores que vêm tentando descrever o seu comportamento através de modelos teóricos. Face à complexidade de descrever estes elementos com apenas bases teóricas, são analisados modelos numéricos e experimentais em estacas cravadas e moldadas no solo exigente da Plataforma Logística de Lisboa.

Devido à importância de uma modelação numérica no dimensionamento deste tipo de estruturas, é analisado um modelo numérico para cada tipo de estaca que são validados através do software PLAXIS 2D. Neste tipo de problemas é essencial para uma boa interpretação dos resultados, perceber a relevância da interface na modelação e de que forma esta pode condicionar os resultados obtidos.

De forma a reproduzir os modelos teóricos e números de ambas as estacas, é feita uma análise de ensaios de caracterização geotécnica como ensaios de penetração standard e de cone. Os modelos reproduzidos são comparados com os resultados obtidos experimentalmente e pelas fórmulas teóricas.

Apesar da quantidade de ensaios realizados ser satisfatória, por terem sido alcançados os valores de carga e deslocamento pretendidos, é necessário melhorar os modelos no ajuste das curvas carga-assentamento, principalmente na fase de descarga. Os resultados da estaca moldada mostraram, serem satisfatórios uma vez que reproduzem uma curva carga-assentamento próxima da curva real. No entanto, os resultados obtidos na modelação da estaca cravada mostraram ter algumas limitações, refletindo a dificuldade que existe em reproduzir todas as condicionantes deste modelo.

Palavras-chave

Estaca, Ensaio de carga Estático, Modelação Numérica, Carga axial, Caracterização geotécnica

Abstract

The analysis of static load test is nowadays essential to understand the behaviour of piles and are there many authors trying to describe its behaviour under theoretical models. Realizing the challenge that is describing its behaviour only by theoretical models, on this thesis are described and analysed numerical an experimental model of driven and bored piles on the from Lisbon North logistics platform.

Facing the importance of the numerical model on the design of such structures, it was analysed one model for each pile using PLAXIS 2D software. On this kind of problems, it is essential to appreciate the role of the model's interface and understand how it can influence the results.

The classification of the soil is obtained by use of simple tests as standard and cone penetration tests. The numerical models are then compared to the theoretical and experimental models. Although the load-displacement curves it is still possible to optimize the models, mostly for the unloading part. The bored pile reproduced quite well the model. However, the driving pile showed to be tough to reproduce, demonstrated all the complexity that it contains.

Key-words

Pile; Static Load Test; Numerical Simulation; Axial load; Geotechnical characterization

TABLE OF CONTENTS

LIST OF FIGURES

LIST OF TABLES

LIST OF SYMBOLS

Latin Alphabet

A_b: Transversal area of the pile base

A_s: Area of the pile shaft

A_k, B_k: Variables dependant of the shear stress of the soil.

c': Cohesion of the soil

C_N: Overburden pressure

c_u: undrained strength of the soil

d: Diameter of the pile

E: Elastic Modulus / Young Modulus

ER_r: energy ratio of Standard Penetration Value (SPT)

$E_{u,28d}$: Elastic Modulus of concrete after 28 days

F_r: Normalized friction ratio

f_s: sleeve friction of the (Piezo) Cone Penetration Test (CPTu / CPT)

I_C: Soil's behaviour type index

K_0: Impulse coefficient

K_S: Earth pressure coefficient

L: Pile Length

l_0: defines the extension of the slip surface

M_{stage}: Multiplier associated with the staged construction process

M: Factor related to the amount of shear strength that is mobilized on the equivalent free surface

N_c, N_q: Capacity Load factor

N_{60}: Number of blows form the SPT.

$(N1)_{60}$: Corrected Value for the SPT

P_a: Atmospheric Pressure

Pb: Load on the pile's toe

Ps: Load on the pile's shaft

Pt: Total Applied Load

q_b: is base resistance per unit of area

q_s: represents the lateral resistance per unit of area

q_t: tip resistance of CPTu

Q_{tl}: Normalized tip resistance

R: Pile Total Resistance

R_b: Pile's base resistance

r_0: radius of the pile

Rs: Pile's shaft resistance

R_f: Friction Ration

s: Value associated to the type of aggregate

w_b: Deslocamento na base da estaca

z: profundity

Greek Alphabet

α: Adhesion's Coefficient of the soil to the pile

α_L: Coefficient dependant of the relation between the length and diameter of the pile

α_E: Modulus factor for estimating the Young Modulus

β: Unit weight (kN/m^3)

β_1: deconfinement parameter

β_w: Unit weight of Water

δ: Friction angle between two different materials (º)

η: angle associated to Janbu proposed slip surface. Also presented on Meyerof slip surface.

λ: Correction factor for rod length

ν: Poisson Coefficient

ϕ': Shear Resistance Angle (º)

σ: Total Stress (kN/m^2)

σ': Total Effective Stress (kN/m^2)

σ_b: Average stress applied by the pile

$\sigma'_{h,0}$: Initial horizontal stress

σ'_0: Total Effective Stress at the pile base (kN/m^2)

σ'_P: Critical Pressure

σ'_Z: Horizontal Stress at depth Z.

τ: Shear stress

τ_p: Passive Shear stress

ψ: Dilatancy angle (º)

LIST OF ACRONYMS

PLLN: North Lisbon Logistic Plattform

SLT: Static Load Test

SPT: Static Load Tes

CPT: Cone Penetration Tests

CPTu: Piezo Cone Penetration Test

1 INTRODUCTION

Planning a Civil Engineering project requires multiple efforts. For instance, to provide a budget for a safe and in-time project deployment, operational efforts are required. Moreover, when an unforeseen event, such as the delay of the required materials occurs, it can harm the due date of the project or bring it to a halt. In case of structural failure due to a bad foundation planning, the consequences can be even worse, contributing to a budget and/or schedule overrun and affecting the safety of the people that work on the construction site or the building.

Therefore, assessing the project requirements and risks is of primordial importance. One of the most crucial phases of the planning is the analysis of the soil's properties. In this thesis, it is explored the theory behind driven and bored piles. These are two commonly used solutions, in many civil engineering works, to support heavy loads, mostly when the structure is founded on soft soils. Due to its importance and to better understand the mechanism for load transfer associated to this type of foundations, it will be explained on the first chapter as well as the bearing capacity theory for these piles.

This Thesis was developed to further explore the theory behind both driven and bored piles and reach numerical approximation, based on situ-test, as well as theoretical analysis.

To recognize the numerical issues, it will be discussed on a full chapter the modelling constrains using two other models to ensure that the output is according to what is supposed to come out from it without distort from the reality. The numerical analysis will be performed by using the software PLAXIS 2D.

The numerical and theoretical will be later discussed on a study case from Lisbon North Logistics Platform (PLLN), close to Tagus. This Geotechnical area is mostly composed by Soft clays what makes it a challenge to design any structure there.

The soil's properties were obtained from several in-situ tests as the Standard Penetrations Tests, Cone Penetration test and boreholes. The data provided from these testes were correlated to the values proposed by some authors and then was analysed according to the results from the numerical, analytical, and in-situ analysis.

These tests are truly important to understand the amount of force that the soil can carry and consequently optimize the design solution not only in terms of safety but also in financial and schedule terms, that takes an important role in every construction.

2 BEHAVIOUR OF A SINGLE PILE UNDER AXIAL COMPRESSION

A pile is a deep foundation, commonly used to prevent unwanted displacements or structure collapses, when such structure is founded on soft soils. When the stiffer layer is several meters building a pile is an efficient method to control the displacements of the structures and the amount of load that the structure can apply on the foundation.

In this chapter are introduced some of the many types of piles that are used in many construction projects and it will be explained some major differences between them. Then, it is explained the theoretical expression to evaluate its resistance. In this chapter are also explained some theories for the pile's toe bearing capacity and its failure surface.

2.1 Pile Types

Depending on its construction method, piles can be divided in two different groups: "displacement" and "non-displacement" piles. At the displacement piles there is no soil removal, since it is displaced radially and axially, as the pile is driven into the ground. In the non-displacement piles, the soil is excavated and extracted by an auger while being replaced/confined or not (depending on if the soil is itself stiff enough to maintain the safety conditions of the borehole).

With the displacement process, granular soils tend to be compacted, and clay soils may heave with small variation in its volume, as long the soil is being displaced. The toe of the pile also compacts the soil in the axial direction (Flemning 2008). The granular soils tend to fill the voids, by getting its particles closer while the clay that have already its particles close to each other, tend to break and heave.

The group of displacement piles can be divided into two subgroups: the subgroup "low displacement piles", described and exemplified by Fleming or Santos (2008), and the prefabricated piles. The first subgroup generally consists of driven small cross-sectional area such as 'H' and 'I' steel piles and open pipes piles. This kind of piles is mostly used in granular soils, at urban centres (induces only low vibrations). The latter induces a much larger displacement It is driven directly into the ground or auger screw piles in which, by use of its helicoidal movement, the soil is pushed out of the axial axis and while it can be, both at the same time or after, filled with concrete.

In the non-displacement piles the soil is normally totally removed from the bore hole. That is when an auger excavates and extracts the soil. If se soils has stiffness enough, the hole is left empty, otherwise it must be replaced by bentonite mud, polymers, or other material, at the same time of the excavation to ensure the safety conditions of the borehole. When the soil is not stiffness enough, the borehole is filled with some fluid such as a bentonite slurry or a polymer fluid, extracted while the concrete is inserted. A steel frame, retrievable or not, can also be used, instead, to hold the ground pressure of the borehole while the concrete is inserted inside. This concrete column may or may not be reinforced. The

boring action of this process may increase the looseness of the granular deposits, and consequently revert the good resistance produced by the compaction. However, it is also true that the concrete of a bored pile tends to create an irregular surface, which improves the load transfer and creates a higher skin friction between the soil and the pile. (Flemming, 2008). On the following table is summarized the several types of pile available in each category of displacement or non-displacement pile. Note that are several different ways to construct piles and every day are putted new solutions on the market.

Table 1- Type of Piles (adopted from (Santos 2010))

<table>
<tr><th>Displacement Effect</th><th>Execution Process</th><th>Material</th></tr>
<tr><td rowspan="4">Large Displacement
(Without soil extraction)</td><td rowspan="2">Prefabricated and driven into soil</td><td>Prefabricated:
• Wood
• Concrete</td></tr>
<tr><td>Closed Pipes:
• Concrete
• Steel</td></tr>
<tr><td>Bored</td><td>Closed Pipes filled with concrete, made of:
• Concrete
• Steel</td></tr>
<tr><td>Auger Screw</td><td>Concrete</td></tr>
<tr><td rowspan="2">Low Displacement
(Without soil extraction)</td><td rowspan="2">Prefabricated and driven into soil</td><td>Steel profiles:
• ‘H’ and ‘I’ sections
• Open pipes</td></tr>
<tr><td>Helicoidal piles made out of steel</td></tr>
<tr><td rowspan="4">No Displacement
(With soil extraction)</td><td rowspan="2">Bored (with pre-sustain)</td><td>Concrete with lost steel case</td></tr>
<tr><td>Concrete with:
• Retrievable case
• Bentonitic Sludges
• Polymers</td></tr>
<tr><td>Bored (without pre-sustain)</td><td>Concrete</td></tr>
<tr><td>Continuous flight augering</td><td>Concrete</td></tr>
</table>

2.2 Bearing Capacity of a Pile

In both displacement and non-displacement piles, their total resistance can be described as the sum of its shaft (R_s) and base resistance (R_b). According to Santos (2008), this relation can be represented with the following expression:

$$R = R_b + R_s \tag{2.1}$$

Furthermore, the base and shaft resistance can be expressed respectively trough the equations 2.2 and 2.3:

$$R_b = q_b * A_b = \left(c \quad * N_c + \sigma_0 * N_q\right) * A_b \tag{2.2}$$

$$R_s = q_s * A_s = (\alpha * c' + K_S * tg(\delta) * \sigma_v) * A_s \tag{2.3}$$

, where:

q_b is base resistance per unit of area,

A_b stands for pile's base area,

c is the cohesion of the soil (c' when drained conditions, c_u when undrained conditions),

σ_0 represents the value of the total vertical stress at the base level (σ'_0 for vertical effective stress at drained conditions),

N_c and N_q are both end-bearing factors dependent of the shear angle of soil and the rugosity of the pile's base,

q_s represents the lateral resistance per unit of area,

A_s is the pile lateral section area,

α is the adhesion coefficient,

K_S earth pressure coefficient,

δ is the friction angle between the soil and the pile (equal 0 in undrained conditions and δ', effective for drained conditions) and, at last,

σ_v is the average vertical stress along the pile's shaft (σ'_v, effective stress, for drained conditions).

The expressions above are equal for both bored and displacement piles. The construction method influences the bearing capacity, and it is expected for the driven piles to have higher values for the shaft resistance, probably due to the densification of the soil in its surrounding.

Although the formula presented for base resistance (eq. 2.2) is quite used by the scientific community, the value of the factor N_c is still matter of discussion. It depends on the way that the pile develops its slip surface at the pile toe. For the factor N_q it is usual to adopt a value of 9 (Santos, 2008).

The following paragraphs will describe a small brief of some of the existent theories that characterizes each slip surface and the correspondent soil's capacity factor for sand, that will be useful to determine the bearing capacity of the piles. Here it will be explored the theories for the load capacity proposed by Terzaghi, Meyerhof and Janbu. There is also introduced one theory for the load capacity only on driven piles, proposed by Berezantzev, Khristoforov and Gulubkov.

2.2.1 Terzaghi

To evaluate N_q, Terzaghi (1943) proposes an equation based on the plasticity theory to evaluate the pile's capacity. According to Santos (2008), the greater difference between Terzaghi and the several other authors that also consider the same theory is the assumption of a value of α equal to ϕ' instead of $\alpha = \pi/4 + \phi'/2$. This assumption makes a huge difference when defining the spiral logarithmic arch CD presented on Figure 1.

Considering the assumption mentioned before, Terzaghi (1943) suggest that the value of N_q can be calculated according to the following expression only suited for when the base of the pile is flat and based on the equations published by Prandlt (1920) and Reissner (1924):

$$N_q = tan^2\left(\frac{\pi}{4} + \frac{\phi'}{4}\right) * \ e^{\pi * \tan\phi'} \tag{2.4}$$

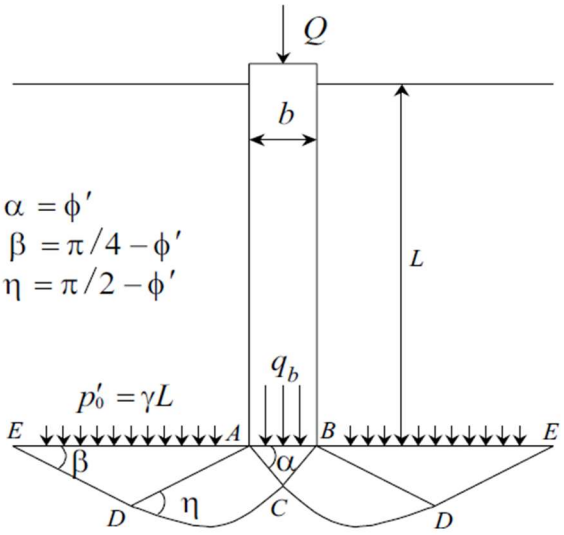

Figure 1- Slip surface proposed by Terzaghi (figure adopted from Santos (2008).

2.2.2 Meyerhof

Meyerhof (1951) assumes that the soil above the pile toe has similar properties from the one where the pile toe is founded, once only that way the soil's contribution can be accounted to the soil's system (Santos (2008)) and he also attributes the capacity to remain in an elastic equilibrium condition and acting as part of the foundation to the triangle 'ABC'. From this triangle, the slip surface starts to develop a slip surface that can be divided in two groups.

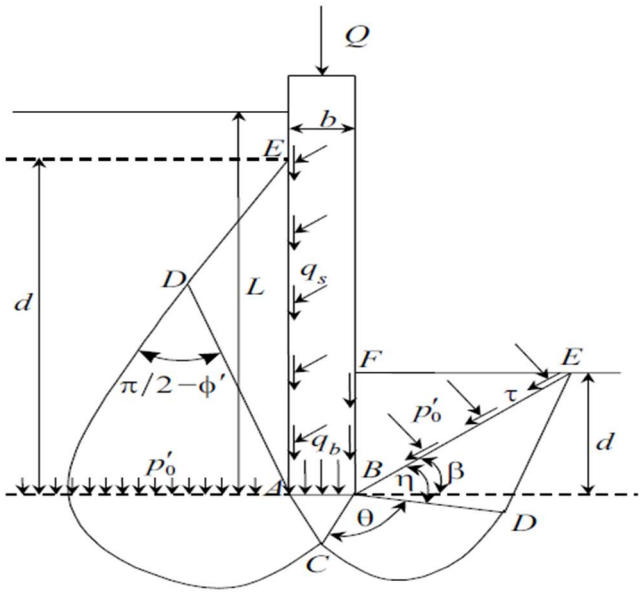

Figure 2- Slip surface proposed by Meyerhof (figure adopted from Santos (2008).

As it is show in Figure 2, the right side shows the surface sliding to the top, reaching the surface, corresponding to a short pile while on the left the slip surface is totally developed without reaching the surface, this case corresponding to a long pile.

he definition between long or short pile is defined by the relation of L/b. If L/b<d/b, the slip surface will reach the surface and the pile is defined as short pile. When the relation L/b is bigger than d/b, the pile does not reach the surface and it is defined as long pile.

Meyerhof (1951) proposes different formulas considering the Mohr diagram (Eq. 2.5), the Mohr Coulomb failure criteria (Eq 2.6) and a factor m (0 < m < 1), characterizing the amount of shear strength that is mobilized on the equivalent free surface.

$$\cos(2\eta + \phi') = \frac{\tau * \cos(\phi')}{c' + \sigma_1' * \tan(\phi')} \tag{2.5}$$

$$\tau = c' + \sigma' * \tan(\phi') \tag{2.6}$$

Where:

$$\sigma_1' = \frac{c' + \sigma_1' * \tan(\phi')}{\cos(\phi')} * [\sin(2\eta + \phi') - \sin(\phi')] + \sigma_0' \tag{2.7}$$

If θ = π/4 – η – ϕ'/2, the surface CD presents a logarithmic spiral form (Prandtl (1920)) and the shearing strength is full mobilized. The normal and tangential components of the passive earth strength mobilized on the surface DB correspond to:

$$\sigma_p' = (\tau_p - c') * \cot(\phi') \tag{2.8}$$

$$\tau_p = (c' - \sigma_p' * \tan(\phi')) * e^{2*\theta \tan(\phi')} \tag{2.9}$$

The bearing capacity can so be defined as:

$$q_b = \sigma_p' + \tau_p * \cot\left(\frac{\pi}{4} - \frac{\sigma_0'}{2}\right) \tag{2.10}$$

If we replace the equation (2.7), (2.8), (2.9) in the equation (2.10), we obtain:

$$q_b = c'\left[\cot(\phi') * \left\{\frac{(1 + \sin(\phi')) * e^{2\theta * \tan(\phi')}}{1 - \sin(\phi') * \sin(2\eta + \phi')} - 1\right\}\right] + \sigma_p'\left[\frac{(1 + \sin(\phi')) * e^{2\theta * \tan(\phi')}}{1 - \sin(\phi') * \sin(2\eta + \phi')}\right] \tag{2.11}$$

Where the terms between parenthesis represent the values of N_c and N_q, respectively.

The magnitude of values of m (0 to 1) have a huge relevance in the bearing capacity factor. If m=0, η=π/4–ϕ'/2 and so N_q equals to:

$$N_q = \frac{(1 + \sin(\phi')) * e^{2\pi * \tan(\phi')}}{1 - \sin(\phi')} \tag{2.12}$$

Otherwise, if m is to 1, then η is equal to zero and so we have N_q equal to:

$$N_q = \frac{(1 + \sin(\phi')) * e^{2(5/4\pi - \phi'/2) * \tan(\phi')}}{1 - \sin^2(\phi')} \tag{2.13}$$

Since those equations can provide values for Nq considered to be too high, Meyerhof (1963) suggested to use the formula (Eq. 2.4) proposed by Terzaghi (1943) in those cases.

To define either is short or long, Santos (2008) compares if relation between L/b is, respectively, lower, or higher than the relation d/b, that can be defined as:

$$\frac{d}{b} = \frac{\sin\left(\frac{\pi}{4} + \frac{\phi'}{2}\right) e^{\pi * \tan(\phi)}}{\sin\left(\frac{\pi}{4} - \frac{\phi'}{2}\right)} \tag{2.14}$$

2.2.3 Berezantzev, Khristoforov and Gulubkov

In 1961 Berezantzev, Khristoforov and Gulubkov introduces a new approach to calculate the bearing capacity of displacement piles. Meanwhile, this theory will differ from the other ones, once is only valid for displacement piles driven on dense sand.

As it was described before, Berezantzev et al. (1963) assumes that the soil that is displaced both in radial and axial directions and that forms compacted zones of soil in the surrounding area and that it has a huge effect in the bearing capacity of a pile.

According to Figure 3, it is possible to identify the shear zones of the soil at the base, showing the compaction of the soil layers resulting of construction process of the pile.

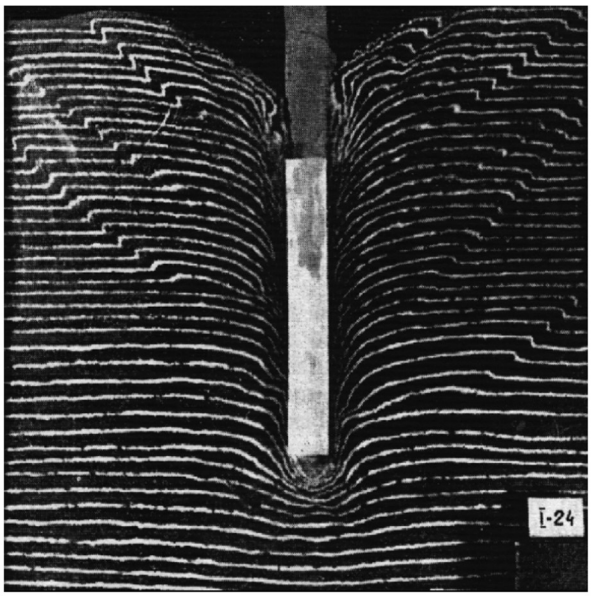

Figure 3- Deformation of the soil soil due to construiction process. Figure adopted from Berezantzev et al. (1961)

The soil's mass resulting from the radial compaction settles the same way as the pile, along the same length (L) with an internal radius that goes from A to B, where the height of that mass starts to be supported by frictional tension developed at the radius B (Figure 4).

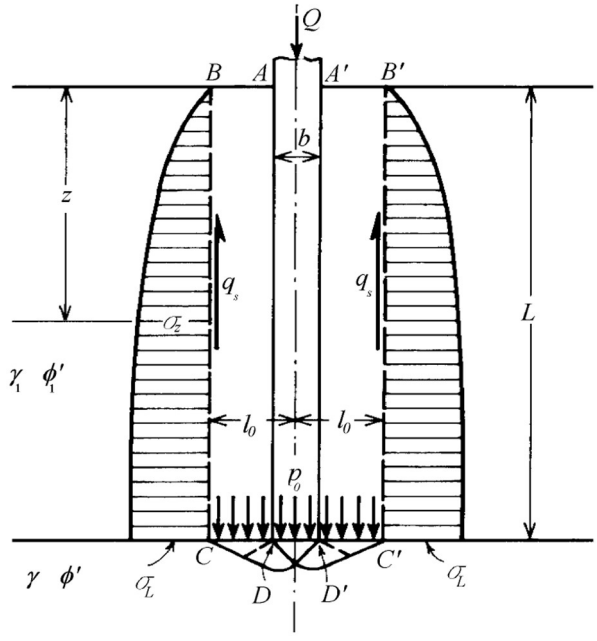

Figure 4- Slip surface proposed by Berezantzev et al. (1961). Figure adopted from *Santos(2008).*

Berezantzev, Khristoforov and Gulubkov suggest that lateral friction can be expressed as:

$$q_s^z = \tan(\phi')\sigma_0 \tag{2.15}$$

And that the horizontal stress at a depth z can be obtained according the following expression, having in consideration the limit equilibrium theory and the axial symmetry:

$$\sigma_z = \frac{\tan(\frac{\pi}{4} - \frac{\phi'}{2})}{\lambda_1 - 1} * \left\{ 1 - \left[\frac{1}{1 + \frac{\tan\left(\frac{\pi}{4} - \frac{\phi'}{2}\right)}{l_0} * \frac{z}{l_0}} \right]^{\lambda_1 - 1} \right\} \Upsilon l_0 \tag{2.16}$$

Where:

σ_z is the horizontal stress at the dept z

$\lambda_1 = 2 * \tan(\phi') * \tan(\pi/4 + \phi'/2)$

l_0 is the soil mass length that can be obtained according to:

$$l_0 = \frac{b}{2}\left[1 + \frac{\sqrt{2}e^{(\pi/2 - \phi'/2)}}{\sin(\pi/4 - \phi'/2)}\right] \tag{2.17}$$

Meanwhile, the expression for the average stress that is applied by the pile results from the equations 2.16 e 2.17 and it can be expressed according to:

$$\sigma_b = \alpha_L \Upsilon L \tag{2.18}$$

Where α_L is dependent of shear strength angle and by the relation between the length (L) and diameter (b), according to the Table 2.

Table 2- Values of αL proposed by Berezantzev et al. (1961)

Φ' / L/b	26º	30º	34º	37º	40º
5	0,75	0,77	0,81	0,83	0,85
10	0,62	0,67	0,73	0,76	0,79
15	0,55	0,62	0,68	0,73	0,77
20	0,49	0,57	0,65	0,71	0,75
25	0,44	0,53	0,63	0,70	0,74

The bearing capacity of the pile footing can be expressed by:

$$q_b = A_k \Upsilon b + \sigma_0 B_k \tag{2.19}$$

Where A_k and B_k are values dependent of the soil's shear stress angle according to the Figure 5.

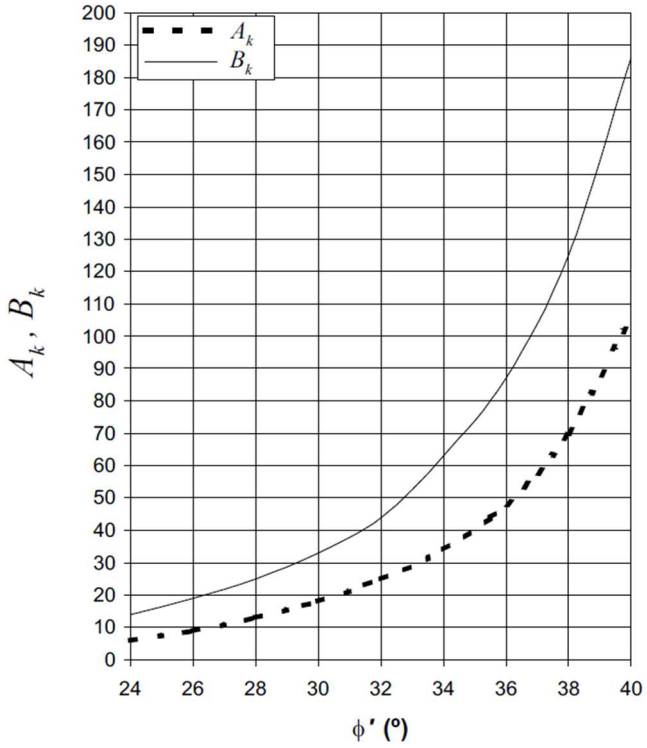

Figure 5- Values of A_k and B_k. Adopted from Santos (2008)

2.2.4 Janbu

Santos (2008) presents the equation to evaluate Nq, according to Janbu (1976). This new equation considers a slip surf as it is shown in Figure 6 and the equation is following:

$$Nq = \left(\tan(\phi') + \sqrt{1 + tan^2(\phi')}\right)^2 e^{2\eta \tan(\phi')} \quad (2.20)$$

Where the slip surface angle η have a value between 70º and 105º if it is a soft clay or a dense sand, respectively.

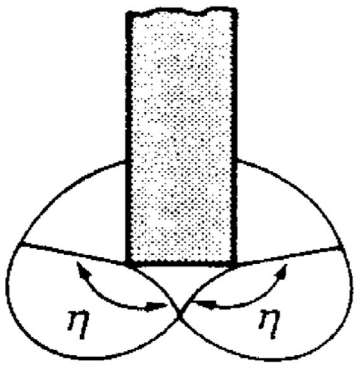

Figure 6 -Slip surface proposed by Janbu (1976). Adopted from Santos (2008)

A higher value for η results automatically in a higher value for N_q and, consequently, increasing the bearing capacity of the pile.

Meanwhile, along this thesis, the theoretical results were obtained according to several authors once it is very difficult to predict the path of tension in the soil and where the plastic points occur, resulting in a slip surface.

The diversity of slips surfaces proposed is since it is impossible to predict with a high level of precision the local where the soil fails and where the rupture occurs. As it was possible to see, this slip surface is heavily dependent of the number of layers, its thickness, soil properties,

Note for the Berezantzev theory that is only applied to driven piles on sand and it tend to result on higher values for the load capacity than the other formulas. This results from the constructive process of driven that induces a particle density increase at the base of the pile that enhances the surrounding soil's resistance. It was adopted a 40º angle of shear resistance for the bottom layer of soil in the calculations of N_q.

3 NUMERICAL VALIDATION OF ELASTOPLASTIC MODELLING OF A SINGLE PILE UNDER AXIAL LOAD

The reproduction of the model using a finite elements software is quite important nowadays once it allows to obtain and reproduce the model much faster than the analytical methods with a high level of reliability, especially when the soil presents many layers of soils and its geometry is complex. The numerical analysis allows to Alyse several results and

However, each model must be verified and tested once that every little mistaken data that is introduced on the model may lead to bad results.

In this chapter it will be discussed the many parameters involved in a numerical analysis using the Plaxis 2D software and some comparisons will be done between the models provided by Ribeiro (2013) and Angelino (2015). This will allow to discuss the many constrains that are involved in such numerical exercise.

3.1 Interface and Loading Properties

3.1.1 Loading

The type of load applied on the pile can be divided in three types: Point load (a and b), distributed load (c) and prescribed displacements (d). Ribeiro (2013) presents four different types of loads applied on a model with a generic geometry of pile and load. From figure 7 it is possible to see that distributed load and displacement gives results closer to the reality and, although the distributed load gives already a good result, it is possible to see that a prescribed distributed displacement can get closer to the real generation of stresses on pile's head and provides better results for the plastic calculation.

The figure 7 was presented by Ribeiro (2013) for load tests applied on a pile with a diameter of 2 meters.

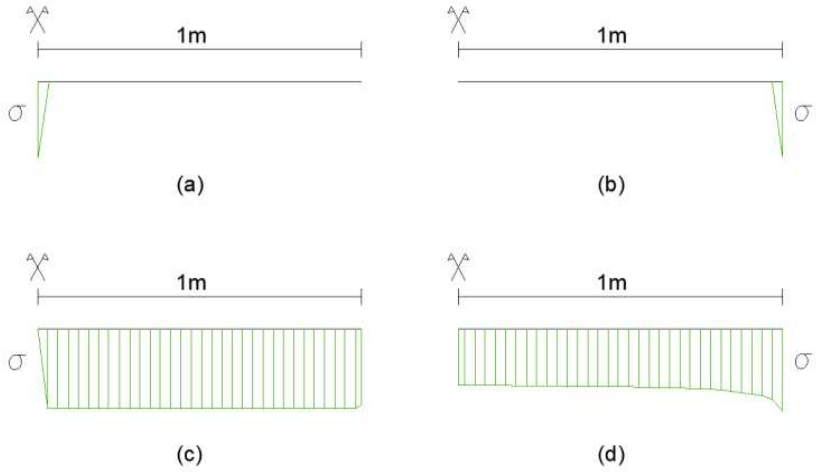

Figure 7- Types of Loading

3.1.2 Lateral Earth Pressure

The initial stresses of the model are highly dependent of the soils weight and the history of its formation. This initial horizontal stress ($\sigma'_{h,0}$) is calculated by using K_0, where K_0 stands for lateral earth pressure coefficient, and its relationship with the initial vertical stress (σ'_0), which is showed by formula 3.1.

$$\sigma'_{h,0} = \sigma'_0 * K_0 \tag{3.1}$$

The value of K_0 can be calculated by three different forms: the K_0 procedure, the gravity loading and Field Stress procedure, that will not be a matter of discussion in the current document. The K0 procedure considers the already referred stress history of the soil and it can only have one value. This value of $K_0=K_{0x}=K_{0y}$, according to Plaxis (2014) manual, is based on Jaky's empirical formula (3.2), independently if it is a normally consolidated or even an over-consolidated soil where the K_0 expression can take another form, based on the consolidation ration, for more complex models.

$$K_0 = 1 - \sin\phi \tag{3.2}$$

When generating stress using this procedure, Plaxis will generate vertical stresses that are in equilibrium with the self-weight of the soil and the horizontal initial stresses are calculated by using the value of K_0 for each type of soil. According to the same manual, this procedure is recommended to use when the

model has on its design only horizontal layers and phreatic level, once that only the equilibrium between horizontal surfaces is ensured.

The Gravity Load procedure calculates the initial stress based on volumetric weight of the soil and, when selected, its self-weight will be the first thing to be applied. This approach takes major importance when using a perfectly plastic soil model such as the Mohr-Coulomb, where the value of the lateral earth pressure coefficient is highly dependent on the value of Poisson's ratio (ν) and the value of K_0 is obtained according to the following expression:

$$\sigma'_{h,0} = \sigma'_0 * K_0 \tag{3.3}$$

$$K_0 = \frac{\nu}{(1-\nu)} \tag{3.4}$$

Both models calculation methods can lead to the generation of plastic points. This can be avoided, on the Gravity Loading approach, by using higher values of K_0, that can be later adjusted, on the following phases of the model, to the real values of the soil.

3.1.3 Interface

To obtain the best response possible from the model it is important to define well the interface properties once it will be essential to understand the amount of load that is carried by the pile's shaft and the part of the load that goes directly to the pile's base.

There are two different factors that are used to define the interface. The first one is the interface's virtual thickness, an imaginary dimension that defines the properties of the interface. This parameter can be manually defined and the higher it is, more elastic deformations will appear on it. This parameter has a default value of 0,1 that can be changed to lower values when the objects are subjected to a large amount of stress.

The second parameter is the strength reduction factor, R_{int}. parameter that defines the amount of the total resistance of the soil that is mobilized. The strength of each layer can be defined according to:

$$c'_{interface} = R_{int} * c'_{soil} \tag{3.5}$$

$$\tan \phi_{interface} = R_{int} * \tan \phi_{soil} \tag{3.6}$$

The value of R_{int} can go from 0,01 to 1 and it should be adopted according to the material. Note that the choice of this parameter value is quite important to account the load that goes to the pile's base or that is dissipated on the pile's shaft. The relevance of this factor on the pile's response can be seen on the practical example present at the end of this chapter.

To exemplify, a bored pile, casted on a sandy soil with a high level of rugosity will have a value of R_{int} close to 1. A driven steel pipe pile with a smooth shaft surface will have a lower value of R_{int}.

3.2 Modelling steps

3.2.1 Definition of the Model

To better understand the constrains when defining a numerical model, it was reproduced a model proposed by Ribeiro (2013). The first stage of modelling is defining the type of model (an axisymmetric model with 15 nodes elements will be used), its geometry (10x20 m^2 model for this example) and its stratigraphy by adding as much boreholes as it necessary to fully define the soil. In the present example, the model is only defined by one borehole, meaning that all layers are horizontal.

The pile is 10-meter-long, with a diameter of 0,4 meters. The five soil layers can be defined in every stage of the model, before it starts running, and its properties are presented on table 3.

Table 3- Soil Properties adopted by Ribeiro (2013).

		L (m)	Material Model	Materyal Type	Y [kN/m3]	c' [kN/m3]	ϕ' (º)	Ψ' (º)	ν	k0	E [kN/m3]
Reinnforced Concrete	Pile	10	Linear Elastic	Drained	24.0	-	-	0	0.3	-	29x106
Soil	Layer1	6,3	Mohr - Coulomb	Drained	16.7	13	26	0	0.12	0.562	9150
	Layer 2	2	Mohr - Coulomb	Drained	18.8	12	23	0	0.12	0.609	13510
	Layer 3	2,8	Mohr - Coulomb	Drained	19.8	14	23	0	0.07	0.609	13570
	Layer 4	8,9	Mohr - Coulomb	Drained	20.0	17	23	0	0.05	0.609	19300

Although the used dimensions, the ideal Plaxis model's geometry should be just as to the one suggested by Randolph and Wroth (1978) where it is recommended that the horizonal distance between the symmetry axis and the vertical limit should be at least 2,0 L once that closer limits may have some interference in the model results. The distance between the surface and the rigid layer should be greater than 2,5 L to ensure that the rigid layers do not influence the amount of displacement of the pile or the amount of load that reaches the pile's base. Ribeiro (2013) suggests areas of mesh refinement based on the pile's radius (r_0), as it can be seen on figure 8.

At this phase, the structures of the models (loads and interfaces) should be defined as well as the limits for the pile's section and the major zones of influence, according to the figure 8.

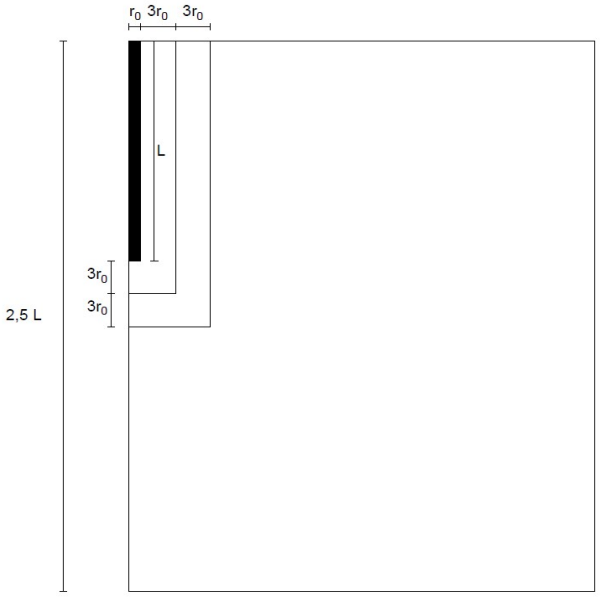

Figure 8- Plaxis generic model's ideal geometry. Ribeiro (2013)

3.2.2 Model's Mesh

Right after the definition of the model's structures, it should be defined the mesh for the model. As said before, it will be composed of triangles with 15 nodes. The mesh will be refined as much as possible, according to figure 8 there are zones where the model is refined, having a higher number of elements corresponding to the zones of transitions between areas, to prioritize zones where the information is much more relevant.

For simpler models, the number of elements can decrease as well as the type of refinement. This can result in not so detailed information, but it can improve a lot the speed of the calculation.

Figure 9- Plaxis 15 nodes elements - Plaxis manual

3.2.3 Groud Water and Seepage Options

Although the information relative to the ground water table can be defined with the borehole, more specific information relative to the water flows is only possible to be defined at this point. In both models presented on this thesis, the seepage options are activated on all boundaries of the model, allowing the water to flow, without generating excess of pore water pressure.

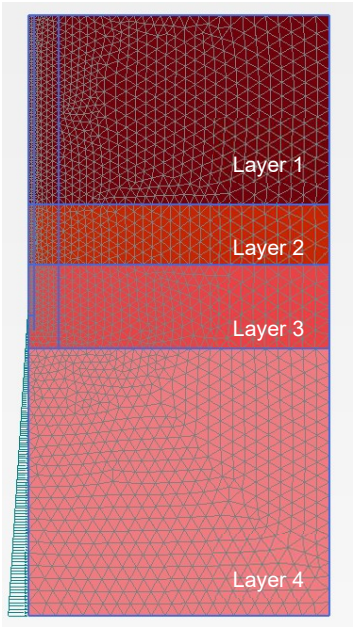

Figure 10- Model's mesh and water presusre diagram.

3.3 Bored Piles

The last stage is the definition of the steps of calculation. As it was explained, first it is defined the procedure to generate the initial stresses. Then, the boundaries of the model should be fully fixed on bottom, horizontal fixed on the laterals and free on top.

After the generation of the initial stresses, the model should simulate the pile's construction process. The part of soil where the pile will fit, will be replaced by the concrete material, with all the interfaces turned off. This will replicate the behaviour of the auger on the soil, implying that the soil around the pile will not be too much disturbed. Then, the interfaces should be turned on, once that in this case all interfaces have different properties than the soil, and the displacements are set to zero. The load/displacement can now be activated and the results from the model can be obtained.

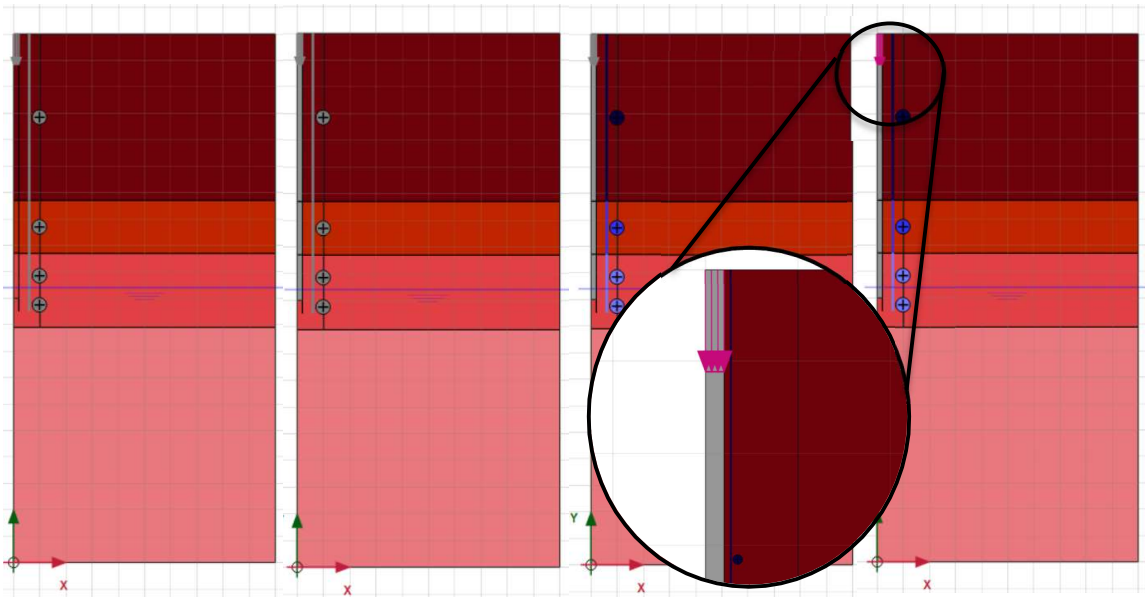

Figure 11- Modelling steps.

Every stage of the model must be analysed to avoid miscalculations and so, the first step is to verify the amount of stress on each layer and see if the values match what was expected. The plastic points should also be verified once that soil must support, at least, its own weight.

After the pile installation, besides of the factors already referred it is very important to analyse the amount of load that is carried by the pile's shaft and base. The total of each parcel should correspond to the self-weight of the pile.

Then, on the last stage, the focus is on the amount of displacement that is applied and the resistance of the pile.

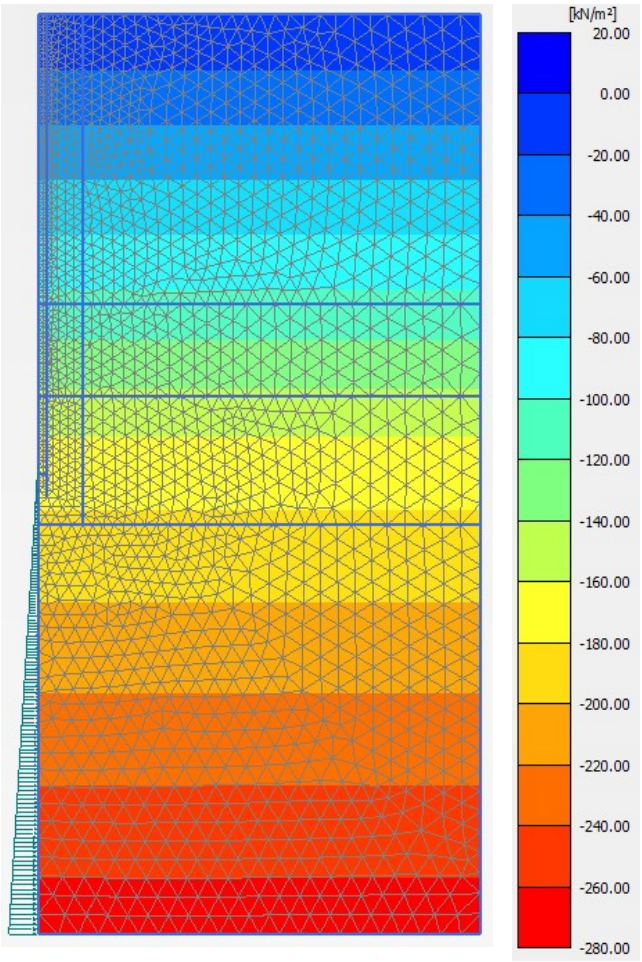

Figure 12- Generation of initial stresses. Vertical Stresses.

For this model, it was performed two different calculations to evaluate the influence that different values for the interface's parameter (R_{int}) have, on the final result, for the load carried by both shaft and pile's base.

A value for R_{int} equal to 0,01, means that the resistance of the soil on its interfaces are only a residual value. The differences between the value presented by Ribeiro (2013) are not significant (but still different), as can be seen on figure 13 or Appendix A1.

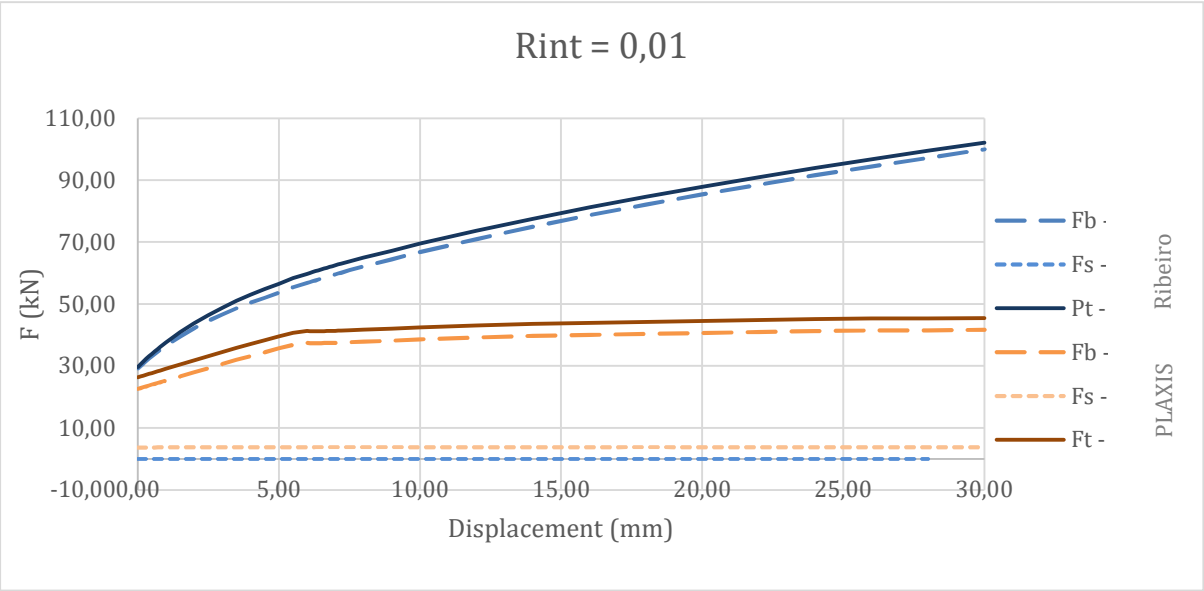

Figure 13- Load-Displacement curves when Rint = 0,01.

On the other side, the values given when the R_{int} is set to 1, are much lower values than the values obtained by Ribeiro (2013) and its comparison of values can be found on Appendix A and on figure 14.

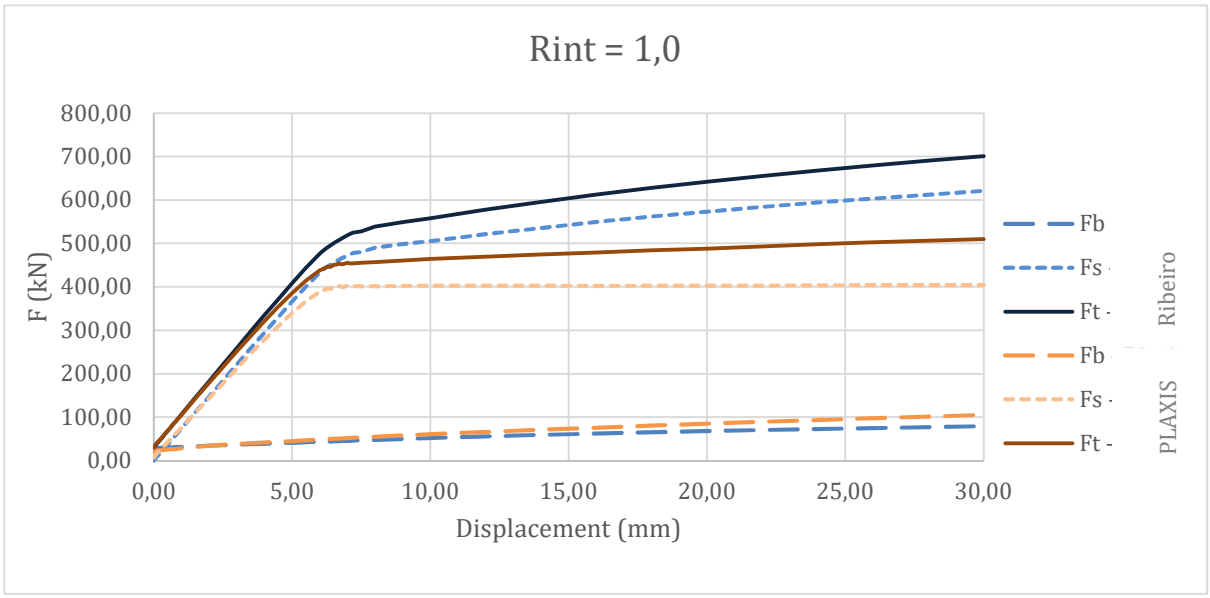

Figure 14- Load-Displacement curves when Rint = 1,0.

It is perceptible the presence of an asymptote on the graph (Plaxis results), which indicates that even for a larger amount of displacement, the soil was not able to accommodate more load on its interface, meaning that the shaft resistance of the soil was already out of its capacity.

According to the figure 13 and 14, the soil's interface capacity describes very well that the results presented by Ribeiro (2013) must have come from a model with stronger properties for some of its layers.

However, it was possible to analyse the difference of values for different R_{int} values. In this case, the full mobilization of the resistance of the soil's interface could lead to values 6 to 10 times bigger than for a R_{int} defined equal to 0,01.

As we can see, this value can lead to a big range of values and so it takes an important role on the material's definition for a correct modelling. It is expected that for layers characterized by it undrain shear strength, the values of R_{int} are bigger than the layers characterized by its drained shear angle.

3.4 Driven Piles

Although it will not be presented any example of a model at these conditions, on this chapter, there are some considerations that are important to state before the case study analysis. The process of the pile's definition follows the same scheme than the bored pile model, However, as it was expected the process for the pile installation is different. As it was explained before on chapter 1, in this case, the soil where the pile will fit will not be removed and so the soil will be radially and axially pushed so the pile can fit in it.

To reproduce this process, Angelino (2015) simulates the process of displacement of the soil by removing the soil's area where the pile should fit and applying lateral pressure on the whole perimeter of the pile and on its bottom. These prescribed displacements are used to simulate the pressure that the ground applies on itself during this construction process. After this process of prescribed displacements, these are turned off and the empty area is activated with the concrete layer.

Although it is not certain the amount of displacement to be applied on, Angelino suggests doing it as an iterative process where the following variables will vary displacement at the bottom, lateral displacement and the Plaxis variable, the $\sum M_{stage}$.

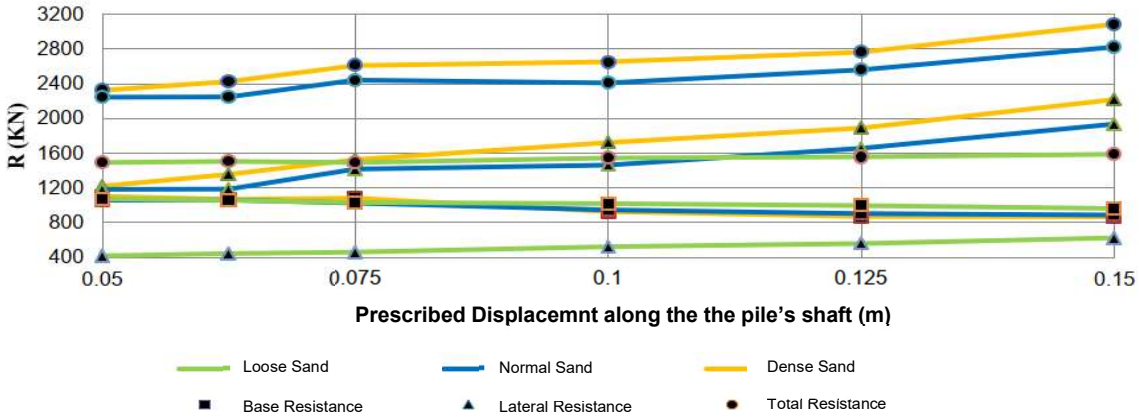

Figure 15- Resistance of the pile according to different prescribed displacements and different kinds of soil, for a 0,360m diameter pile. Adopted from Angelino (2015).

The amount of displacement is not yet easy to determine but its definition takes an important role on the results of the model. And while it may vary a lot between models, the amount of displacement applied on the base of the pile is generally bigger than the amount applied on the pile shaft. As shown on Figure 15, the amount of lateral displacement prescribed on the soil will give a bigger value for soil resistance in its global, but the base resistance may reduce a bit. It is also possible to understand from the same figure that the effect of soil prescribed displacement is more significant on dense sand.

The $\sum M_{stage}$ factor is a multiplier associated with the staged construction process. This factor allows the software to move to the next stage without ending the current one. When defines to a value lower than one, the ultimate level of the phase is not finished, and it will be ended on the following stage, although the following step have to be calculated as *Staged construction*. This tool allows to better control the process of removing the soil and the appliance of prescribed displacements without the soil's body collapse. This follows the same principle of the construction a NATM tunnel, where the forces around the empty hole are calculated by use of the expression $(1-\beta_1)$. According to the Plaxis (2006), β_1 can vary between 0 and 1 an it is a deconfinement parameter, that relates the cluster inside the tunnel that is retained as support pressure.

Also, according to the experience of Angelino, the value for the $\sum M_{stage}$ has an important role in the resistance of the pile. In this case, when the pile has less stages of calculation, i.e., lower values of $\sum M_{stage}$, the pile can mobilize more resistance. While the shaft resistance tends to be higher due to tension state that is related to the residual tension that s created on the pile shaft during the contraction of the cylindrical cavity, the base increases just a bit of tis resistance due to the increase of shaft resistance (Angelino (2015)).

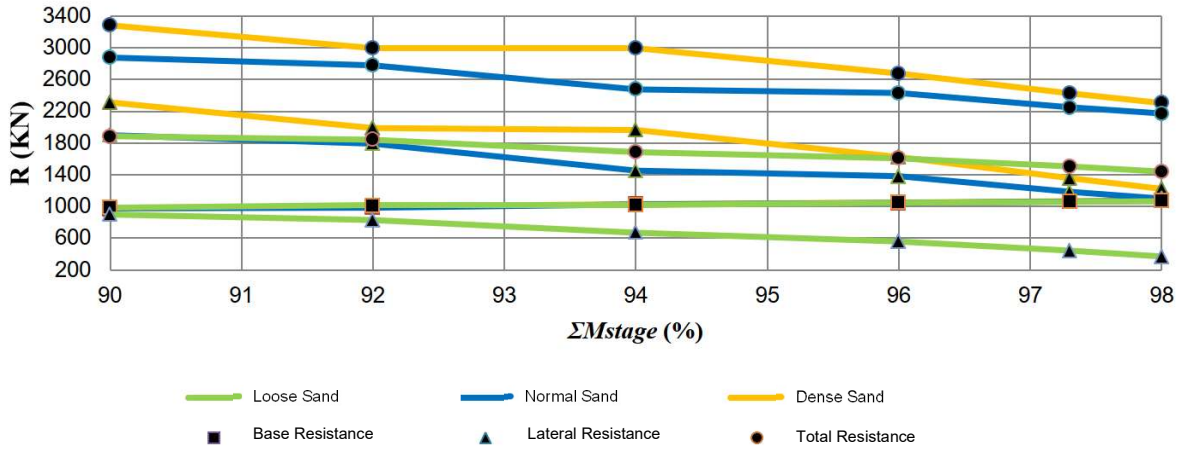

Figure 16- Pile's resistance with the variations of the multiplier $\sum M_{stage.}$ - Angelino (2015).

Meanwhile, one of the limitations of Plaxis 2D is the impossibility to represent a square section pile. To overcome this problem, it is recommended to adopt a circular base pile with a value for it radius that allows the pile to have the same length and the same shaft area, so the resistance of its shaft and base can be evaluated.

4 CASE STUDY - LISBON NORTH LOGISTICS PLATFORM (PLLN)

It is intended to build several warehouses to be working mostly as logistic centres at Lisbon North Logistics Platform (PLLN), located at Castanheira do Ribatejo. This location is known to be part of the wetlands of Tagus River, being mostly composed by soft clays and a high level of the water table.

The Static Load Test are used mainly to optimize the adopted solution on the PLLN foundation. Instead of working with the most common tests, this static load tests allow to understand better the response of the soil and estimate a reduction on, for example, the piles length. When adopting shorter piles, the cost of the project can reduce significantly.

All ground investigations works were adjudicated to the Portuguese constructer Mota-Engil, SGPS, S.A.

Figure 17- Localization of the case study.

4.1 Lithology and Soil Characterization

To characterize the indicated site, several tests as Boreholes with soil samples collection, Standard Penetration Tests (SPT) and Cone Penetration Tests (CPT) were performed to evaluate the properties of each layer of soil until the 40 meters deep.

The indicated area was already matter of interest some years before and so it has already been subjected to a previous consolidation. This consolidation was performed by the application of stone columns and a 3-meter landfill over the field. This work has been mapped and the following tests were performed to obtain the response of only the soil itself without any disturbance of the preview stone columns work. The over consolidation ratio is registered to be between 0,6 -1 on the first 17 meters and 1-2 between 19 to 24 metres of depth.

Since the zone nearby the river is the most unfavourable sector of the site, the Static and Dynamic Load Tests were performed at the “S1” location and therefore, the soil’s characterization tests mentioned

before took place at the indicated localization. Although zone S1 is referred as the most important to characterize the soil, it Is obvious that the characterization tests were carried away on many other points of the site. In total were performed 2 boreholes, 2 CPTu and 40 boreholes with SPT tests.

4.1.1 Boreholes

Although this kind of test may seem simple, it is essential to know and understand the soil's layers distribution. The soil profile was extracted by use of a rotational drilling machine.

Figure 18- Soil's Profile. Result from the extraction of the borehole close to the Static Load Tests. (Mota-Engil Fundações (2019).

It can be seen the 3 meters, already referred above, of the posterior embankment followed by almost 14 meters of muddy clay soil. From 17,40 to 19,5 it is showed some coarse silt sand followed by almost 5 meters of silty-sandy clay. At the 24 meters deep appears a 4-meter layer of fine to coarse sand that is interrupted at the 28 meters deep by a thin layer of mud with clay and fine sand. From the 30 meters the soil goes from fine sand to coarse sand and therefore to pebble with big dimensions. Excluding the first layer.

4.1.2 Poisson Coefficient

Once this coefficient can be only obtained by some laboratory tests and these were not performed, it was assumed that the Poisson Coefficient (υ) has a value of 0,3 for soils characterized by its drained shear strength angle and a value of 0,5 for soils characterized by its undrained strength.

4.1.3 Standard Penetration Test

As well as the boreholes, the Standard Penetration Test (SPT) is probably the most used technique worldwide once it is fast, allows to get the stratigraphy of the soil and it has a low-cost when compared to some other tests. Although it is more reliable to characterize sandy soils, it is also used in cohesive soils since it can quickly provide some information about the type of soil.

The values of the number of blows required to settle 30 cm of soil were registered in situ every 1,5 meters of deep and then they were corrected to the real value of the test. It was used a machine with an energy ratio of 60% (ER_r = 60), a correction factor for rod length (λ) between 0,75 - 1,0, depending of the deep of the excavation, and a value of the correction for overburden pressure (C_N), where the reference pressure is the atmospheric pressure (P_a = 101,3 kPa) (Liao & Whitman (1985)).

$$N_{60} = \frac{ER_r}{60} * N \tag{4.1}$$

$$(N1)_{60} = N_{60} * \lambda * C_N \tag{4.2}$$

Where C_N can be obtained according to:

$$C_N = \sqrt{\frac{P_a}{\sigma_0}} \tag{4.3}$$

The unit weight of the soil was estimated using the correlation proposed by Bowles (1971).

The correlations between the undrained shear strength or the angle of shearing resistance and the number of blows of the SPT were proposed by Terzaghi & Peck (1967) and Meyernof (1956), respectively.

Even though the SPT is not the best solution to characterize the Young modulus (E) of the soil, Kulhawy and Mayne (1990) propose several equations to evaluate the elastic modulus of the soil, depending on its type of soil and suited well more to granular soils.

For sands with fines or fines:

$$\frac{E_s}{Pa} = 5 * N_{60} \tag{4.4}$$

For non-consolidated clean sands:

$$\frac{E_s}{Pa} = 10 * N_{60} \tag{4.5}$$

For over-consolidated sands or gravel:

$$\frac{E_s}{Pa} = 15 * N_{60} \tag{4.6}$$

At the deep of 31,5m, it was impossible to obtain any values of the STP once at that deep it was found pebble, making it impossible to perform such test.

Table 4- SPT and its correlation

Z(m)	N60	γ(kN/m3)	σ (kPa)	σ' (kPa)	λ	CN	$(N1)_{60}$	c_u (kPa)	ϕ' (º)	E (MPa)	Geotechnical Zones
0	-		0	0	0,75	-	-				
1,5	-	19	28,5	28,5	0,75	-	-	-	28 - 30	18	Sandy Fill
3	18		57	57	0,75	1,333	18				
4,5	-		79,5	64,5	0,85	1,253	1				
6	-		102	72	0,85	1,186	1				
7,5	-		124,5	79,5	0,95	1,129	1				
9	-		147	87	0,95	1,079	1				
10,5	-	16	169,5	94,5	0,95	1,035	1	< 20	-	0,5	Muddy clay
12	-		192	102	1	0,997	1				
13,5	-		214,5	109,5	1	0,962	1				
15	-		237	117	1	0,930	1				
16,5	-		259,5	124,5	1	0,902	1				
17,4	15		273	129	1	0,886	13				
18	15	20	282	132	1	0,876	13	-	32 - 35	15 - 25	Coarse silty sand
19,5	26		312	147	1	0,830	22				
21	11	19	342	162	1	0,791	9	150 - 250	-	5 - 15	Silty-sandy clay
22,5	24		370,5	175,5	1	0,760	24				
24	50		399	189	1	0,732	37				
25,5	*52*		427,5	202,5	1	0,707	37				
27	60	21	427,5	187,5	1	0,735	44	-	36 - 41	90	Fine to coarse sand
28,5	*48*		427,5	172,5	1	0,766	37				
30	26		459	189	1	0,732	19				
31,5	*60*		490,5	205,5	1	0,702	42				

Accounting the effects of gravel column, the soil should be characterized by a higher value of Elastic Modulus instead of the ones provided by the SPT. This can be checked while analysing the results o the CPT, that is more suitable when correlating the parameters of the soil.

4.1.4 Piezo-Cone Penetration Test

The Piezo-Cone Penetration Test (CPTu) is a very important test to characterize the foundation's soil. From this test it is possible to obtain the point resistance (q_t), the side friction (f_s) and the pore water pressure (u) and, with that information it is possible to make several correlations for the soil is properties as well as its deformation modulus, shear angle resistance and undrained shear resistance.

The results provided by the company are shown on figure 19, where it can be seen the first 24 meters and a *Soil Behaviour Type* chart, where it is described the type of soil for each value obtained from the test.

From the figure 19, and already making correlations with the previous results, it is possible to see that the soil can be divided in 5 principal layers. The first one, corresponding to the sand embankment, goes from the surface until 3 meters deep and it is characterized by values for the tip resistance near of 2 MPa. The second layer, corresponding now to the soft clay that reaches 17,0 meters, show values around 0,5 MPa for the upper layers of clay that will increase to 1 MPa near 17 meters. From 17,0 to 19 meters, it is shown higher values for the point resistance that may vary between 2,5 to 20 MPa, showing a stiffness increase. The 4th layer presents lower values again and its tip resistance has values of 1 to 3 MPa. The last layer that appears at 24 meters, shows a big increment in is values for q_t and f_s, at least, higher than 15 MPa for the point, showing some agreement with the previous tests.

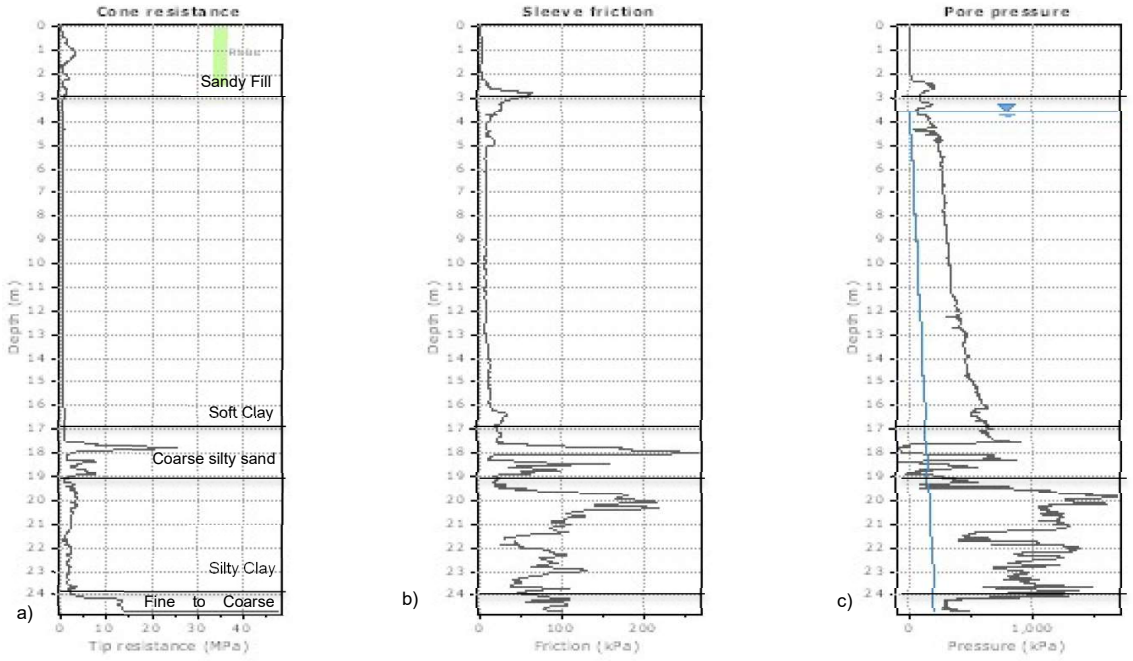

Figure 19- Variation of Point and Shaft resistance and pore water pressure. a) q_t; b) f_s; c)u. - (Mota-Engil Fundações (2019).

Robertson (2010) introduces the expression 4.7 that can correlate the unit weight of the soil considering the values of sleeve friction (f_s) and tip resistance (q_t), obtained in the test.

$$\frac{\Upsilon}{\Upsilon_w} = 0{,}27 * \log(R_f) + 0{,}36 * \log\left(\frac{q_t}{P_a}\right) + 1{,}236 \tag{4.7}$$

Where:

P_a is the atmospheric pressure with a value of 101,3 kPa.

R_f is the Friction Ration that can be obtained according to the following the expression.

$$R_f = \frac{f_s}{q_t} * 100 \tag{4.8}$$

The Soil Behaviour Type's chart (presented in Figure 20), introduced by Robertson (1990), allows to classify the soil according to its resistance in 9 possible groups, according to soil's normalized friction ratio (F_r), that is expressed by equation 4.9 and represents the relation between the point and the normalized tip resistance (Q_{tl}).

$$F_r = \frac{f_s}{q_t - \sigma_{v0}} * 100 \tag{4.9}$$

$$Q_{tl} = \frac{q_t - \sigma_{vo}}{\sigma'_{v0}} \tag{4.10}$$

As it was expected, the soil is mostly classified as being of "clay to silty clay" type, with silty sand layers at the top and at intermediate layers. At the limits of the CPTu it is found "Clean sand to silty sand".

Once the soil type is identified, it is possible to correlate deformation and resistance values with the values presented above. For the layers where the soil was defined by its undrained resistance, it was adopted the equation proposed by (Kulhawy and Mayne 1990), where N_{kt} represents a coefficient with values between 10 and 20, depending on if it is a soft non-consolidated or an over-consolidated clay, respectively. Robertson and Cabal (2015) suggests adopting a value for N_{kt} equal to 14.

$$\frac{-\sigma_{v0})}{N_{kt}} \quad (4.11)$$

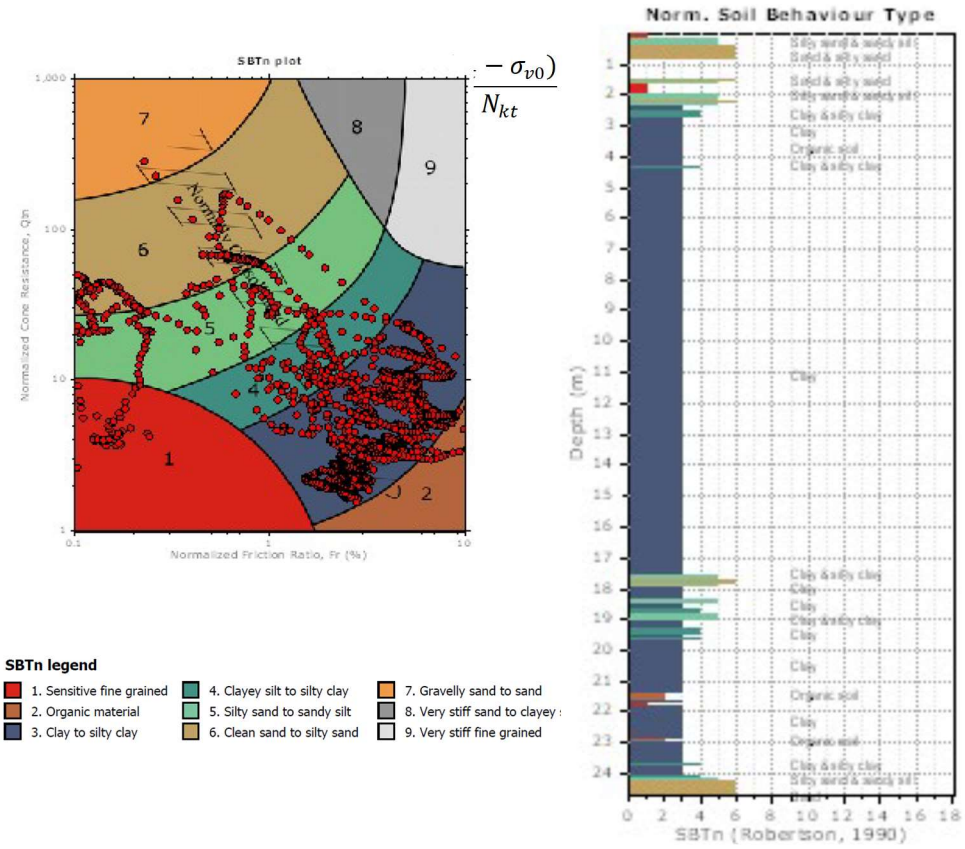

Figure 20- Soil's Behaviour Type. - (Mota-Engil Fundações (2019).

On the other hand, for sandy layers of soil, the shear angle resistance can be described according to equation 4.12, formulated by Robertson and Campanella 1983, with the Kϕ and Cϕ being coefficients approximately equal to 0.1 and 0.37, respectively.

$$\tan(\varphi') = K_\phi + C_\phi \log\left(\frac{q_t}{\sigma'_{vo}}\right) \quad (4.12)$$

To fully describe the behaviour of the pile in terms of deformation, it is also very important to have some correlation to the soil's elastic properties. The response of the pile is directly corelated to the Elastic

Modulus and to the poison's coefficient. To define the value of E it was used the following correlation proposed by Robertson (1990):

$$E = \alpha_E(q_t - \sigma_0) \quad (4.13)$$

Where α_E is the modulus factor for estimating the Young's Modulus and it can be estimated from the value of the soil's behaviour type index, I_C:

$$\alpha_E = 0.015 * 10^{0.55I_c+1.68} \quad (4.14)$$

Where I_C is equal to:

$$I_C = \sqrt{(3.47 - \log Q_{tl})^2 + (\log F_r + 1.22)^2} \quad (4.15)$$

Table 5 summarizes the all the soils properties resulted from the CPTu.

Table 5- CPT soil's properties

Geotechnical Zone	z (m)	q_t (MPa)	q_s (kpa)	Ɣ (kN/m^3)	c_u (kPa)	ϕ (º)	E (MPa)
1	0 – 3	≈ 2	≈ 50	19	-	30 - 33	25 - 30
2	3 – 17	≈ 0,5	≈ 20	15	30 - 75	-	7-50
3	17 – 19	2,5 – 20	75 – 200	20	-	34 - 38	70 - 90
4	19 – 24	1,0 – 2,0	50 – 150	19	100 – 150	-	60 - 80
5	24 – ∞	15 - 50	≈ 100	21	-	40 - 45	130 - 160

On the following calculations, the adopted model is:

As It was expected, due to the high proximity of tests, both shows very similar results. Since the CPT obtains values continuously and not only every 1,5 meters (as the SPT), the values on the table 6 were adopted both on the numerical and analytical solutions.

The procedure of this test follows the same principles than the one performed on chapter 2. The model is still an axisymmetric model with elements of 15 nodes. Although the recommendation mentioned on chapter 2, the model is 60x30, ignoring the recommendation of having a model 2,5 times longer than the pile, but assuring that does not affect the results.

The model is then defined by 6 following layers of soil, according to the results of the tests. Note that the Geotechnical Zone 3 comes from an abrupt increase of the 2nd layer soil's strength but maintaining the clay profile.

Note that the numerical analysis requires some adjustments that are obtained in an iterative process and so the soil's properties comes from the crossing of the various tests that were performed.

Geotechnical Zone 1 (GZ1):

The first layer of soil is a 3-meter depth layer of very loose sand (volume weight with values of 10 to 30 blows by the SPT and with an Elastic modulus value of 5 to 20 MPa. The CPTu also indicates a point resistance bellow 3 MPa. It was adopted a unit weight of 19 kN/m^3, a friction angle of 32º and an Elastic Modulus of 35 MPa. R_{int} is equal to 0,62 and k_0 is by default, 0,470, according to expression 3.2.

Geotechnical Zone 2 (GZ2):

This 11m thick layer with a unit weigh of 15 kN/m^3, due to its weak properties, is not able to handle any blows from the SPT and, as it was expected, have a point resistance under 1 MPa. As it is usual to happen with most clays, the soil it is characterized by its undrained behaviour and its c_u has a value of 30 kPa that increases linearly to 60 kPa. Its Elastic modulus is equal to 5 MPa and it has a Poisson's coefficient of 0,499. Its interface mobilization factor is 0,8 and its k_0 is 1,0.

The stone columns and the pre-load works increase the consolidation of the soil and so they are reflected on the Elastic Modulus of hist layer, resulting in a stiffer geotechnical zone.

Geotechnical Zone 3 (GZ3):

The stiffer layer of clay has higher values of resistance ad it is characterized in the model with the same unit weight of the previous layer (15 kN/ m$^{3)}$, a c_u of 75 kPa, an Elastic Modulus value of 40 MPa and a Poisson's coefficient of 0,499. The value of R_{int} is equal to 0.9 and k_0 is 1,0.

Geotechnical Zone 4 (GZ4):

The stiffer clay has now an undrained resistance of 54 – 136 kPa, properties that results of a point resistance 1 – 5 MPa and 8 – 15 blows from the SPT. The soil is defined with γ = 20 kN/ m^3, ø' = 32º, E = 70 MPa, v = 0,3. The value of R_{int} is equal to 0,64 and the value of k_0 is 0,441.

Geotechnical Zone 5 (GZ5):

From values of 8 to 15 blows and a q_t =3 to 7 MPa obtained from the SPT and CPTu respectively, this soil layer is defined with γ = 18 kN/ m^3, c_u = 120, E = 55 MPa, υ = 0,449. The value of R_{int} is equal to 0,9 and the value of k_0 is 1,0.

Geotechnical Zone 6 (GZ6):

For last, on the bottom we found a stiffer layer, with blows above 50 and a confined point resistance above 10 MPa. From these results it is possible to extrapolate the following characteristics: γ = 21 kN/m^3, E = 130 MPa, υ = 0,3 and ϕ' = 36º. For R_{int} and k_0 were defined values of 0,6 and 0.412, respectively.

For every layer that was defined by its shear strength angle, it was also defined a value of cohesion of 0,01, this does not make any difference on the result but it's important to be defined so the model can run.

4.2 Bored Pile

4.2.1 Experimental Model

Pile execution and installation

The works for the construction of the bored pile occurred between May 22 and May 27 2019 and it started by performing the excavation with buckets and an auger, digging a deep hole that was held up using ben bentonite sludges. The verticality was assured by the short case placed on the top on the excavation. While the excavation process, the hole was maintained stable by use of bentonite sludge.

Figure 21- Bored Pile is Static Load test

Then, on the 34m long and 800 mm diameter pile, several strain gauges were installed, 3 per one of the ten levels and this equipment recorded the compression/extension at each level. On the top was placed LVDT (Linear Variable Differential Transformer) displacement sensors and a load cell sensor. The concrete used on the pile was class C35/45.

Procedure

The Static Load Test on the bored pile took approximately 33 hours to be performed. It started at midnight of May 3rd, 2019 and lasted until 11.20 AM of May 4 2019.

The objective of this test was reach at least 2 times the maximum service load, 5600 kN. The increment of load was 700 kN for each step and the test reached 2800 kN at first and then the load was unloaded to 0. It was again loaded until it reached the final load of 5600kN.

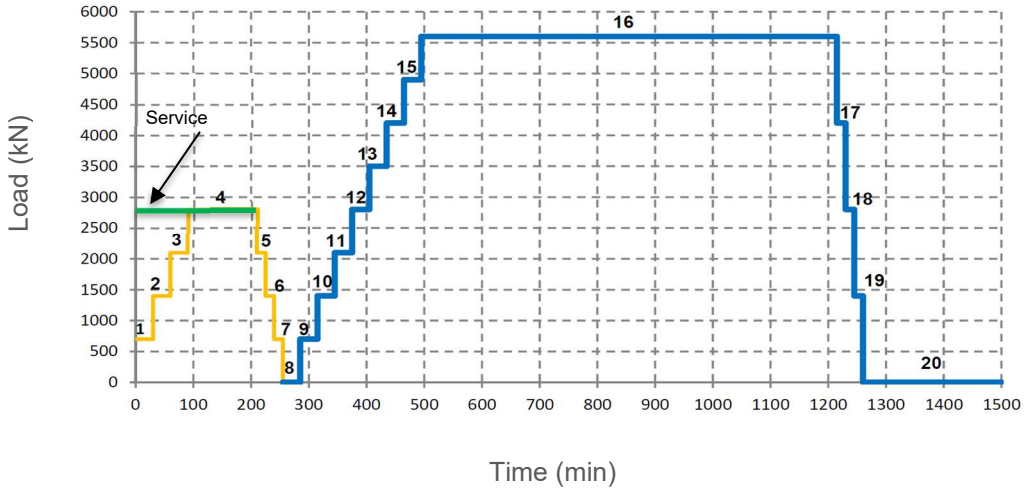

Figure 22- Static Load Test Plan – Bored Pile. - Mota-Engil Fundações (2019).

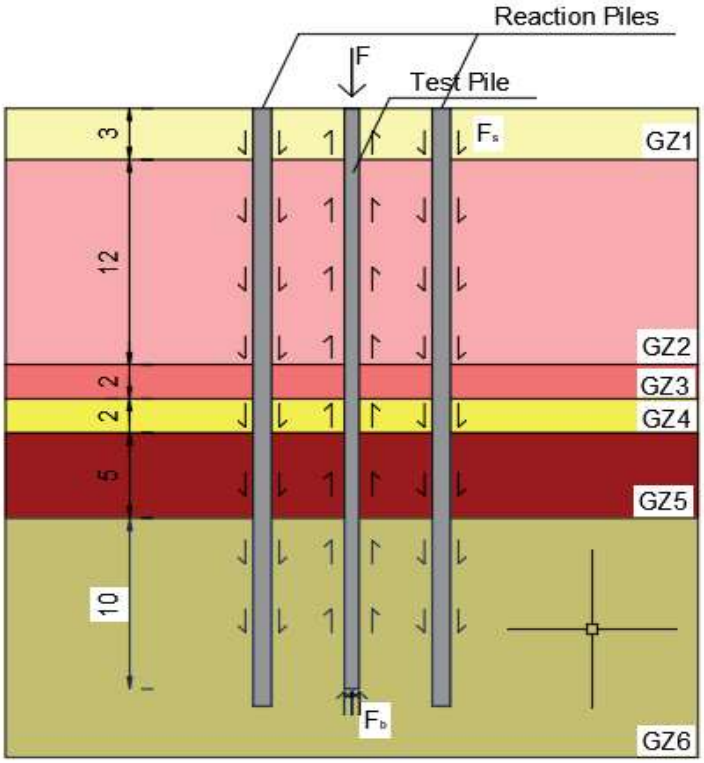

Figure 23- Bored Pile Scheme.

The load applied to the pile was performed by using a hydraulic jack which created a vertical reaction when used against a steel structure connected to what is called reaction piles. This steel structure was connected to 4 bored piles with 40m length and 1m diameter. These 4 piles were only subjected to traction forces.

Results

To obtain the real values of the test and since that the pile was tested only eight days after it was casted, the value for the Young Modulus (E) was adjusted according to the expression proposed by *Eurocode 2*.

$$E = E_{u,28d} * \sqrt{e^{s\left(1-\sqrt{\frac{28}{t}}\right)}} \quad (4.16)$$

Where:

s is value depending on the type of aggregate used, 0,2 in this case (for limestone);

$E_{u,28d}$ is the value for the young modulus of concrete at 28 days, 30MPa, for the concrete of class C35/45.

For the type of concrete already referred, the value of the Young Modulus is 27,5 MPa.

From this test, it is possible to obtain two important graphs that can explain the behaviour of the pile. The first one presented (figure 23) is the load-settlement curve, where it is observed the amount of load carried by and the respectively displacement measured on the top of the pile.

It was also possible to obtain the information about the amount of load caried by each level of strain gauge that were placed along the pile. Meanwhile this information will be discussed later o this thesis since it requires additional information from the theoretical and numerical results to better interpret the results.

Yet, the results do not figure the variation of the Young Modulus that is not constant the whole test, and it changes abruptly, especially under higher values of force.

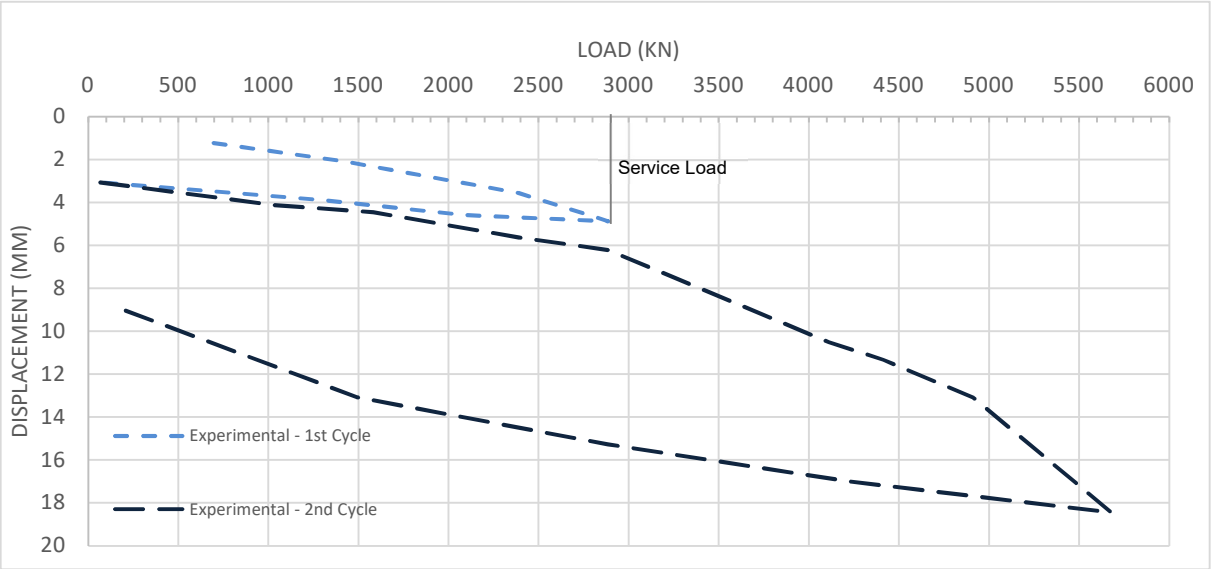

Figure 24- Load-Displacement curve - Bored Pile Head

4.2.2 Numerical Model

Model, soil, and elements properties

The concrete of the pile differs from the Mohr-Coulomb material model applied on the layers and its behaviour is calculated using a linear elastic model.

Note that for a numerical approach, the value of the shar strength had to be adjusted, starting with a low value and increasing in depth. Otherwise, the soil would collapse, and the numerical run would stop.

This information is summarized on the following table.

Table 6- Soil's Model Properties.

GZ	Material Model	L (m)	γ (kN/ $m^{3)}$	c_u (kPa)	ϕ'(º)	E (MPa)	υ	R_{int}	K_0
1	Mohr–Coulomb	3	19	-	30	35	0,3	0,62	0,47
2	Mohr–Coulomb	12	15	30-60	-	5	0,499	0,8	1,0
3	Mohr–Coulomb	2	15	75	-	40	0,499	0,9	1,0
4	Mohr–Coulomb	2	20	-	32	70	0,3	0,640	0,44
5	Mohr–Coulomb	5	18	120	-	55	0,499	0,90	1,0
6	Mohr–Coulomb	10	21	-	36	130	0,3	0,62	0,41
Concrete	Linear Elastic	34	25	-	-	30 *10^3		1,0	1,0

No interface was defined on this model once it is not totally clear what other values would it have. The interface's weaker properties were defined only by the factor R_{int}.

The value of R_{int} on the model was defined assuming that it has a high level of rugosity, also created by the small variation on its diameter all along the pile, increasing that rugosity. This follows the principle enunciated on chapter 3.

The water level was defined at 3,3 meters deep.

Calculation

The mesh was defined with a high level of refinement, especially on the most sensitive areas, close to the interfaces of the soil layers. There were also defined the transition areas according to the example on chapter 3. This resulted on a model with 4015 elements, 32591 nodes.

The calculation steps follow the same approach than the one used on chapter 3, with the only difference being the interface non-activation, this meaning that only the parameters related to soil's resistance were adjusted (using the tool R_{int}).

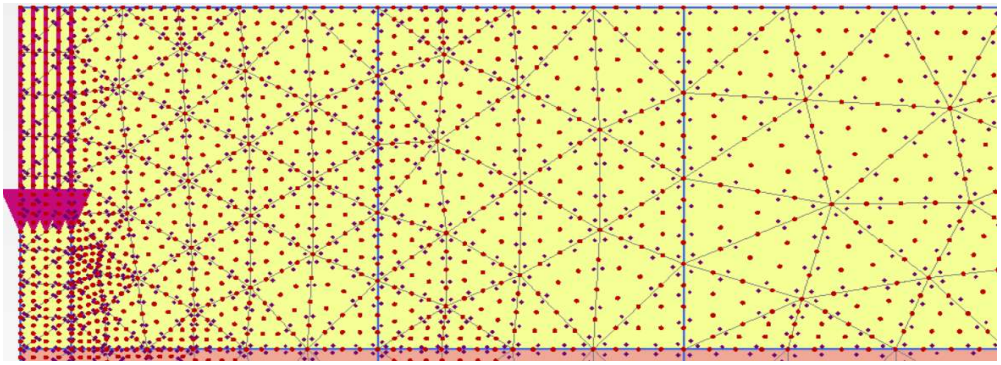

Figure 25- Model's mesh refinment.

The initial stresses were generated according to the K_0-procedure calculation without the pile layer yet attributed. The second phase correspond to the cast of the pile, replacing the equivalent layer of soil with concrete properties. After this, the displacements and strains were put to zero and the test began.

The load was applied in terms of displacement instead of force, according to the model proposed by Ribeiro (2013) and the test was performed under the 21 steps.

Results

The global behaviour of the pile is presented on figure 26, where it is shown the evolution the load on the pile and the displacement associated to this. This type of graph is the sum of all particularities that are happening in the soil and in the model. It easy to identify that the behaviour of the experiment and the behaviour of the model have big differences between them, although the total load applied, and the

stress carried by their shafts are similar. It is also possible to observe on figure 27 the amount of load carried by the pile's shaft and the piles base, validating the amount of displacement prescribed.

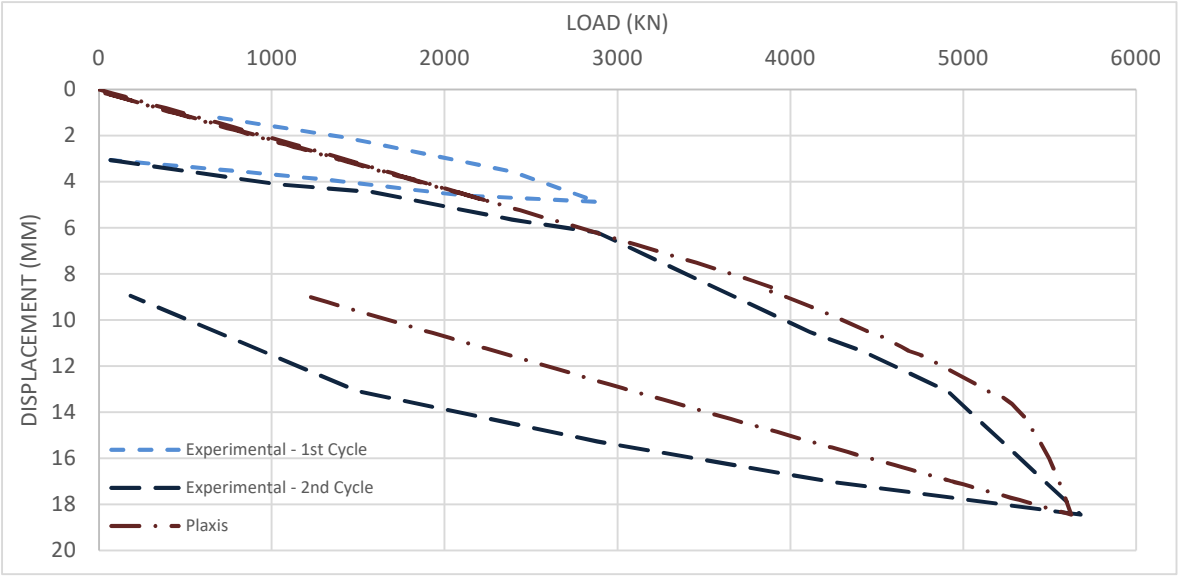

Figure 26- Bored Pile's Load-Displacement Curve.

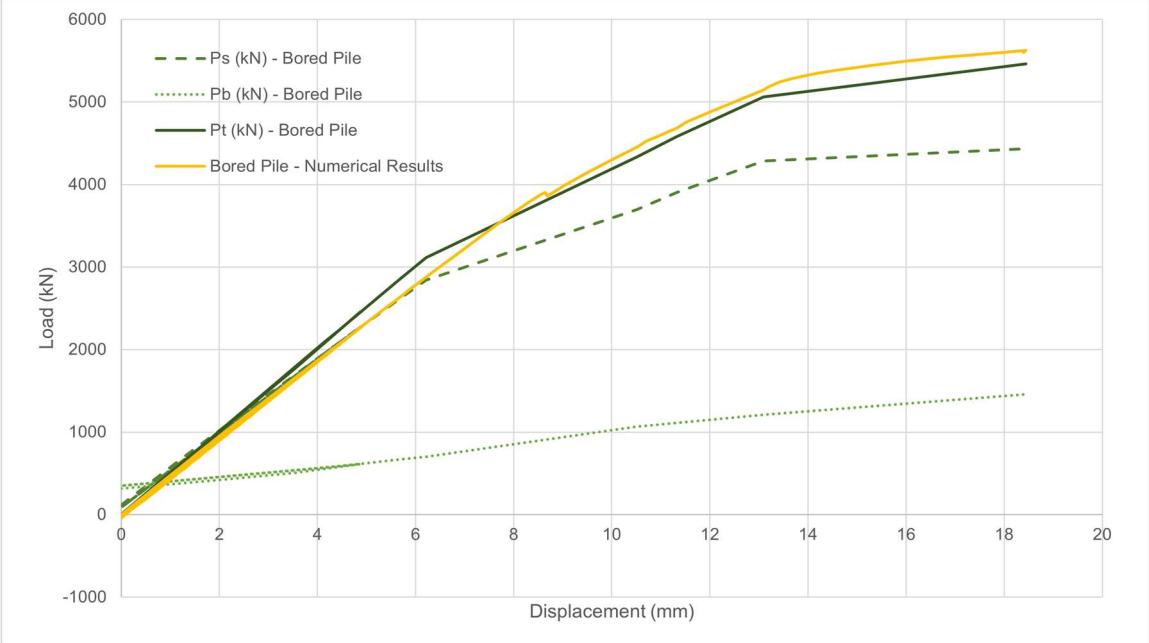

Figure 27- Amount of load on the pile's shaft and on pile's tip under the axial compression. - Numerical Analysis.

4.2.3 Overall Remarks

The results provided by full scale load test were clear enough to understand the pile's both shaft and base mobilized resistance.

During the installation process of the pile, the strain gauges that are allocated along the rebars can be lost due to the several impacts that may occur during the casting or during the movement of the pile is concrete reinforcement. This may, sometimes, induce errors to the result provided by the extensometers.

This time was no different and the three extensometers on top the pile, corresponding to the 10th level of strain gauges, were damaged making impossible to count with these values. Along the other levels, several extensometers were spoiled and that made values of certain levels not so reliable. The number of strain gauges working on each level are indicated in both figures 28 and 29, where the red font indicates that only one extensometer worked, yellow for two and green when all strain gauges worked fine.

Looking at the figure 27, it is possible to understand, on a first glance, that some mistake has occurred, during the test or during the information processing, once that it is not possible to have the lower extensometers (SG06 and SG05) subjected to a bigger load than the upper strain gauges (SG08 and SG07).

Many reasons can explain this or, at least, some discrepancy of the values. The mentioned loss of some strain gauges may be responsible for some of the result's variability.

Even that it was no possible to have access to the amount of concrete spent on the pile's casting nor the sonic tests results, the main reason for this discrepancy of values can be attributed to the variation of the pile's cross section. In both figures 28 and 29, it is possible to identify the five layers of soil where is possible to figure where the soil contracts or expands. When casting the pile, it is very common for the soil to contract (where sandy soils fill the hole) or to expand, when the concrete expands radially, filling the surrounding weak soil's space. This theory may be one of the cases for the unexpected behaviour of cells 08, 07, 06 and 05. Sometimes this cross section new configuration can be detected by a sonic test.

The change on pile diameter is he explanation for the lower force results on the upper levels because it was assumed that there was no generationof negative friction forces on the pile shaft.

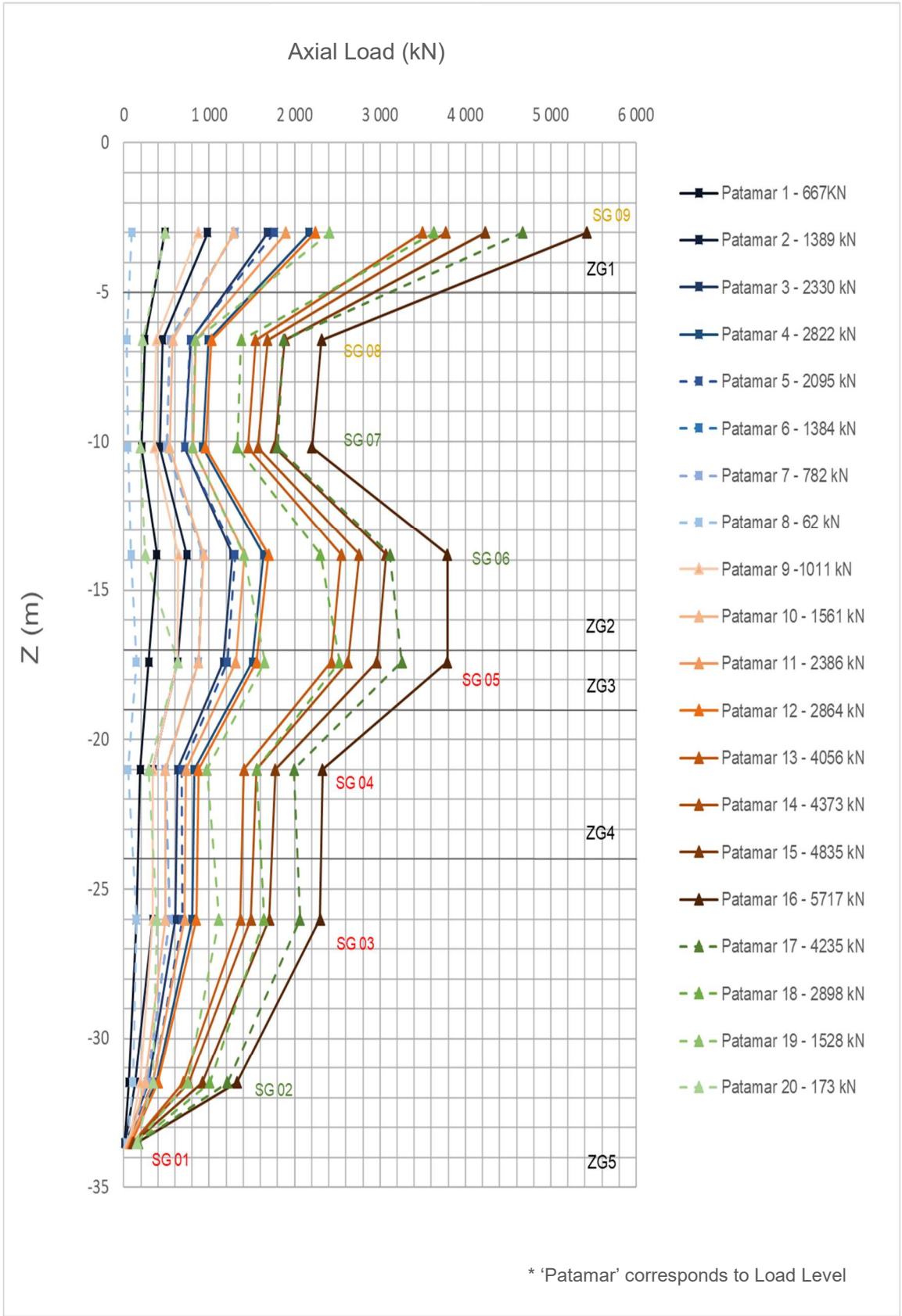

Figure 28- Amount of Load carried on each level of extensometer.

The force on each is highly dependent on the diameter of the pile as it can be seen on equation 2.2. The strain gauges 08 and 07 were placed at the level of the weakest layer of soil while the extensometers 06 and 05 are in stiffer layers of the soil. In that case, it was adopted for the first two strain gauges diameters of 1,0 m while, for the 05 and 06, it was adopted values of 0.75 and 0,7 meters, respectively.

Table 7- Proposed Diameters.

LEVEL	D
SG9	0,8
SG8	1
SG7	1
SG6	0,75
SG5	0,7
SG4	0,8
SG3	0,8
SG2	0,8
SG1	0,8

During the numerical and theoretical analyses, it was also possible to evaluate the state of the 10th strain gauge since it does not sense almost any stress. The total pile's shaft resistance was estimated to be close to 4500 kN and the graph presents only a minimal force on that level. Note that the total amount for the shaft load is calculated by subtracting the total load applied by the amount of load given by the last strain gauge. To better adjust this value, it was added a line, on the same alignment that SG02 and SG03 and so the estimated load carried by the pile's shaft and base is 4600 kN and 1000 kNm respectively.

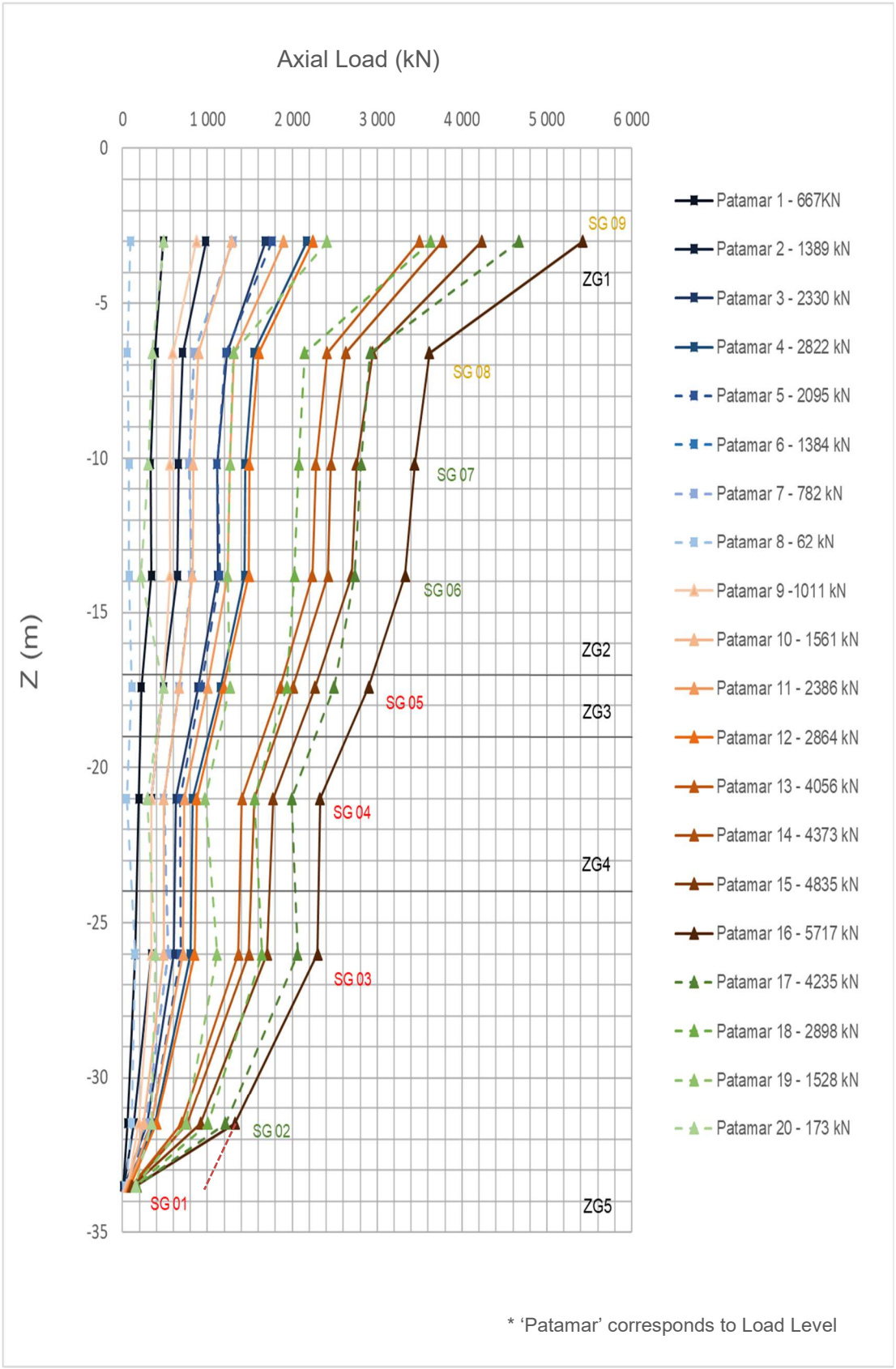

Figure 29- Proposed Correction of the Amount of Load carried on each level of extensometer.

Shaft resistance

Using the same parameters as the ones used on the numerical analysis, it was possible to estimate the shaft resistance of the pile, based on equation 2.3.

Table 8- Shaft resistance of the Bored Pile.

Z (m)	σ ; σ' (kPa)	σmed (kPa)	ϕ'(º)	δ (º)	c_u (kPa)	K_0	q_s (kN/m)	R (kN)	Total (kN)
0 3	0 57	28,5	30	0,367	-	0,5	5,5	41,35	4499,9
3 15	57 237	147	-	-	40	-	40	1206,4	
15 17	237 267	252	-	-	75	-	75	377	
17 19	130 150	140	32	0,394	-	0,470	27,4	137,8	
19 24	307 397	352	-	-	120	-	120	1508	
24 34	190 300	245	36	0,451	-	0,412	48,9	1229,4	

From the three possible analysis to evaluate the shaft resistance, it was clear that the shaft resistance is almost the same for every calculation, although that does not mean that the numerical model is correct, once it was calculated by using the already referred iterative process and because the numerical model does not reflect completely what happened on the field.

Base Resistance

It was not matter of this test to reach the full capacity of the pile but to understand its behaviour. However, the base resistance of the pile can be estimated, and it slip surface evaluated. To calculate the bearing capacity of the pile, it will be used the formulas enunciated for the authors present on chapter one. Note also that the equation proposed by Berezantzev will be not used because it only refers to driven piles.

Since the pile is not loaded to its full capacity (nor even close to that), the estimation for the bearing capacity will be only performed by approximating the numerical model slip surface to the ones proposed.

Table 9- Bored Pile's toe resistance.

Base Resistance						
Theory		**N_q**	**σ_0**	**q_b (kPa)**	**A_b (m2)**	**R_b (kN)**
Terzaghi		19	607	11271	0.5	11271
Meyerhof	m=1	370		224601		112897
	m=0	38		22916		11519
Jambu	η = 70	23		13799		6936
	η = 90	38		22916		11519
	η = 105	55		33523		16851

It is impossible to estimate the value of the bearing capacity of the pile, however it can be estimated by the numerical model. As the figure 30 shows, the total capacity of the pile is much higher than the one applied during the static load test. The total capacity of the pile is 11.483 kN for a prescribed displacement of 38 mm. Although it hard to estimate, the lower slope (figure 25) of the experimental pile indicates that the bearing capacity may be higher than the one obtained by the numerical model.

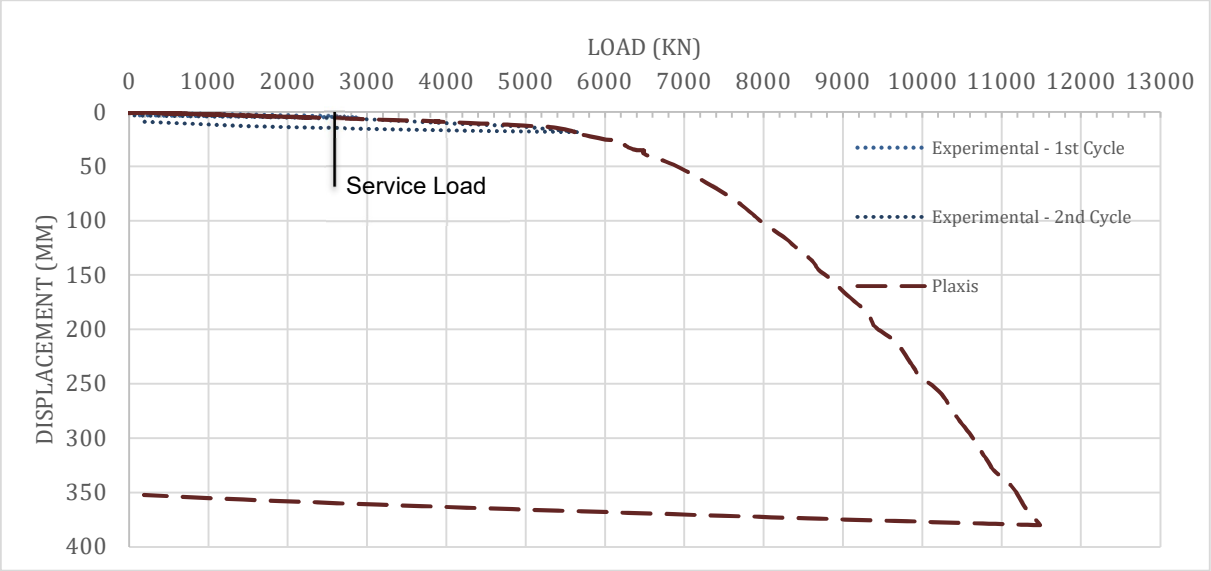

Figure 30- Failure on numerical model for a displacement of 38mm.

One good option to estimate the bearing capacity of the pile's toe is by analysing the plastic point development. In fact, the plastic points are formed on the piles base and they tend to extend to the bottom and to the surround are of the piles toe. The slip surface proposed by Terzaghi is right put aside once its value is estimated only based on the shear angle of the soil and, facing the estimated 36º for

the shear angle for the last layer, slip surface would develop mostly in the radial direction rather than the axial direction of the of the pile's toe.

This gives two options; the toe capacity of the pile may relate to the Janbu proposed slip surface for medium/low values of η since the smaller this angle is, more the slip surface develops on the axial direction of the pile. For this option, the pile's toe capacity cannot be lower than 6936 kN. Although on the numerical model it was possible to estimate values that go higher than that.

The last option leaves us with the Meyerhof theory that proposes a wide range of value for the bearing capacity. As described on chapter one, the value m is related to the angle η. When m is equal to 1, η is 0 therefore, this option is put aside. This implies that the bearing capacity of the pile must be lower since the pile's toe does not expand on the radial direction. However, it is quite difficult to estimate one value.

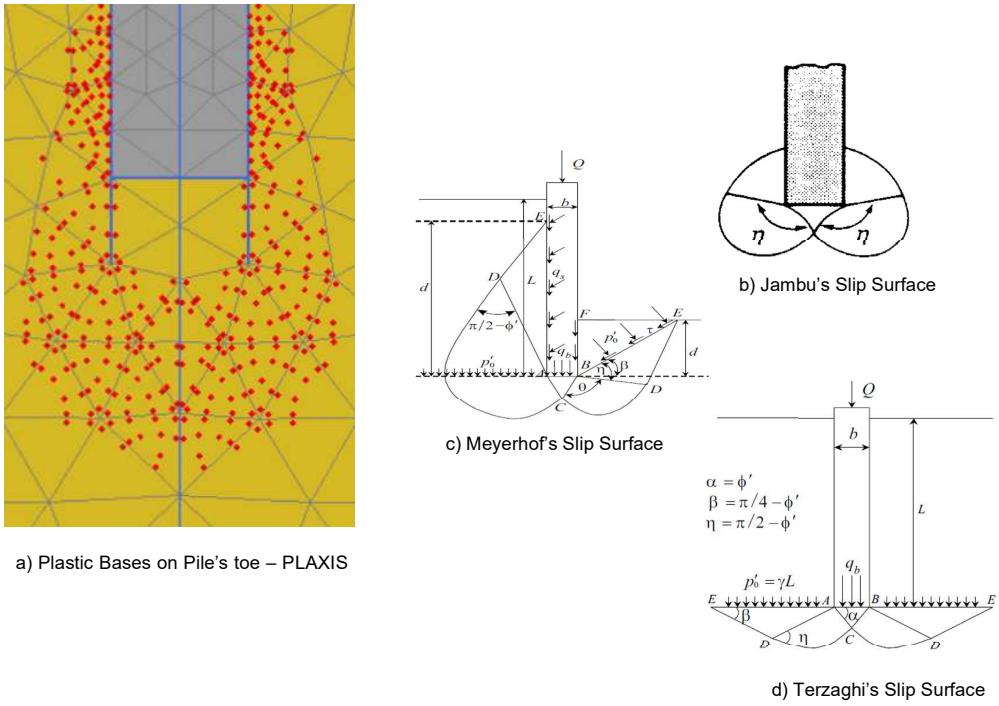

a) Plastic Bases on Pile's toe – PLAXIS

b) Jambu's Slip Surface

c) Meyerhof's Slip Surface

d) Terzaghi's Slip Surface

Figure 31- Comparation between slip surfaces and the pile toe under an axial force of 5600 kN.

4.3 Driven Pile

4.3.1 Experimental Model

The driven pile had square section of 400mm with 31.8 meters long, with a steel connection between its segments. It was inserted on the ground by use of an automatic hammer and right after its installation on the ground, a test based on wave propagation verified the pile's integrity.

During the installation process, it was possible to feel the waves on the ground of the hammer hitting the pile. When the pile reached the big layer of clay soil, it was seen that the pile slipped inside the soil several meters without any effort.

The 31,8m square section of 400m driven pile was tested on April 29 and April 30, 2020 and the aim of this test was to apply three times the total service load expected to be on this structure. First, it was applied a load until it reaches 1200 kN, proceeded by a total discharge, then it was applied a total load of 3600 kN that was unload at the end. It is interesting to observe that the same pre-cast pile is limited up to 2300 kN by the Terratest catalogue. The assumption of a lower service load (1200 kN) may be related to the slenderness of the pile and to prevent excess on the magnitude of the moment that an eventually eccentricity may cause.

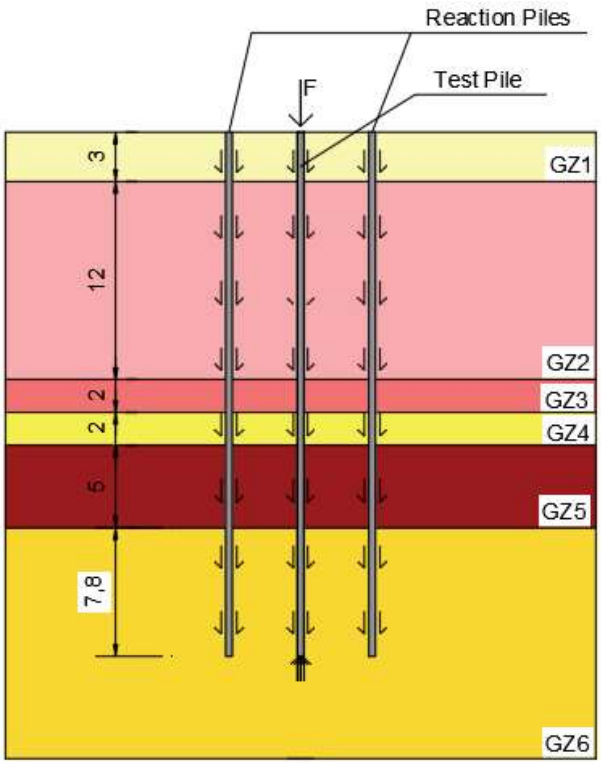

Figure 32- Driven Pile Scheme.

A system composed by a structure, rigid enough to prevent any undesired settlement of this structure, was used to place the six dial gauges used to measure the displacements of the pile head.

Figure 33- Static Load Test Performed on the Driven Pile.

To apply the load, it was used a hydraulic jack, a hydraulic pump, and a manometer that, together, reacted against to a steel structure, transferring the load to another 8 driven piles with same dimensions as the one from the test.

When observing the load-displacement curve (Figure 34), we can see that for the final step of load, the displacement increases without raising the amount of load. This indicates that the pile increases its plastic behaviour, although it does not necessarily mean that the pile is in its full capacity.

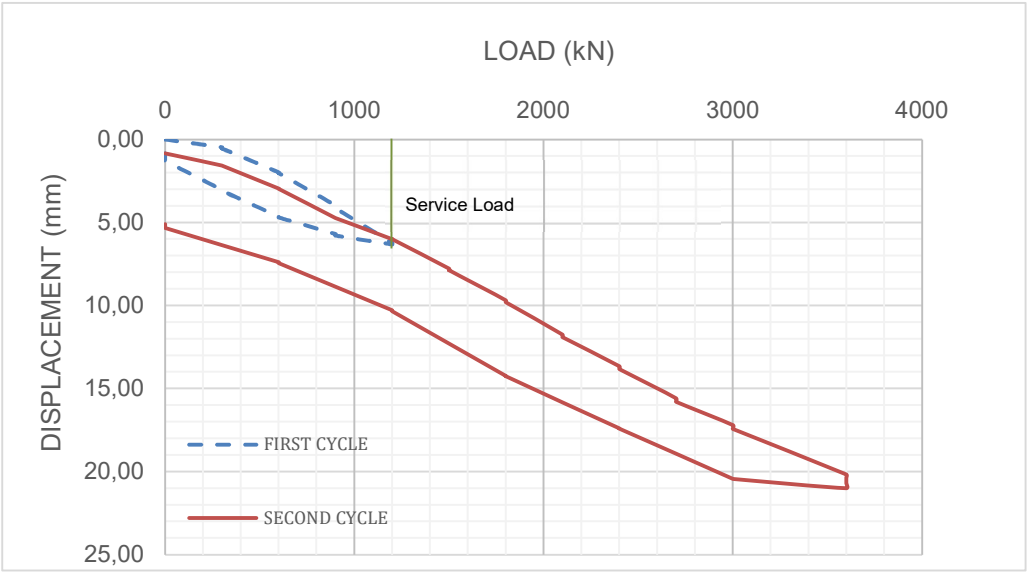

Figure 34- Experimental Load - Displacement curve of the driven pile.

4.3.2 Numerical Model

The Plaxis model followed the same principles as the methods introduced on chapter 3. The model of the soil is identical to this one, although the process of the pile introduction is somewhat different involving some model's structures that were not applied on the bored model. The mesh was refined the same way that it was on the last examples, resulting on a mesh with 4919 elements, 41083 nodes. The water table remained the same, 3,3 meters under the surface.

The numerical model is an axisymmetric model and so, the 0,4 meters square section pile, will now be one pile with the same 31.80 meters length and with a circular section with a diameter of 0,5 meters. This allows to maintain the bottom of the pile in same level of the ground, with same lateral areal and with a small increase of the cross-section area.

To better control the pile's interface, this time it was necessary to define an interface structures with a new range of elastic values for the soil that would complement the typical reduction of the strength properties already used on the bored pile (table 10). However, it is important to remember that the goal was to maintain the soil properties according to the reality.

Table 10- Strength and Elastic reduction of the Driven Pile Interface.

	GZ1	GZ 2	GZ 3	GZ 4	GZ 5	GZ 6
R_{int}	0,40	0,9	0,8	0,7	0,8	0,5
E (MPa)	15	1	25	50	20	70

As showed on chapter 3, to simulate the introduction of the pile it was necessary to add load displacement structures. Although, unlike the model proposed by Angelino where he prescribes displacements over the model's interface at once, this time, the pile is introduced step by step so it can get closer to the real process of installation, by applying displacement on 2 or 3 meters of soil by step. It was adopted 10 steps to insert the pile on the ground. The displacement was reseted (like it was done on the bored pile model) so it was possible to obtain the displacement from the test.

The lateral displacement was defined to 0,035 m (0,07 D) and a base displacement of 0,15 m (0,3 D). The base's displacement showed to be determinant on the magnitude of the shaft resistance. When a lower displacement is applied on the pile's base the shaft resistance tens to get bigger. However, not matter how much or lower the value of the resistance gets, the soil's load – displacement curve does change, almost recovering to its initial state.

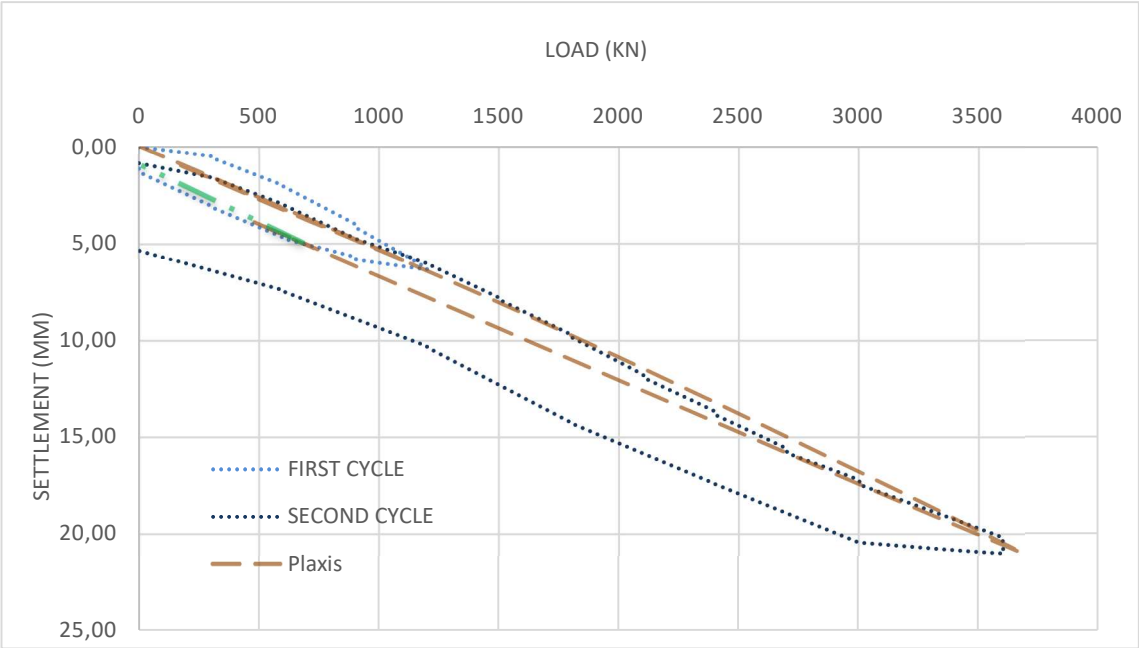

Figure 35- Load - Displacement curve of the Driven Pile Head - SLT.

The numerical analysis was performed to have the same amount of load applied equal to the one applied on the field and trying to replicate the test and its construction process without losing the attention on maintaining real soil's properties. However, this model showed to be hard to control the stresses on the pile with so many parameters that may influence the behaviour of the pile under stress,

By the graphic analysis (Figure 34), its clear to see that although the pile's displacement is achieved for the same amount of load prescribed on the experimental test, the pile does not show any signal of reaching nor the pile's shaft capacity and, consequently, not the pile's base capacity. However, when comparing both load – displacement curves (considering the second cycle) the curves are very close to each other, between numerical and experimental models.

Still talking about the Plaxis curve, in fact, when unloading (see the green extension represented on Figure 35), the pile shows almost no signal of permanent deformation, recovering almost its initial form, with a permanent deformation of only 1 or 2 millimeters. The reason for this difference may be due to the prescribed displacements during the construction process that induce undesired (or unrealistic) stresses on the pile's interface. Other reason can be the excess of resistance on the pile's interface parameters, even after the significant reduction when compared to the bored pile.

In fact, as it demonstrated on figure 36, the process of radial displacement induces a lot of stress on the surrounding soil of the pile, creating a big area of plastic bases and taking an important role on the shaft resistance of the pile. For this reason, and as it was described before the interface demonstrated a huge importance on the mobilization of stress of the pile's shaft.

It is also important to refer the discontinuities of plastic points that are possible to observe on Figure34, it happens on the transition of layers due to the significant difference between the stiffness of layers.

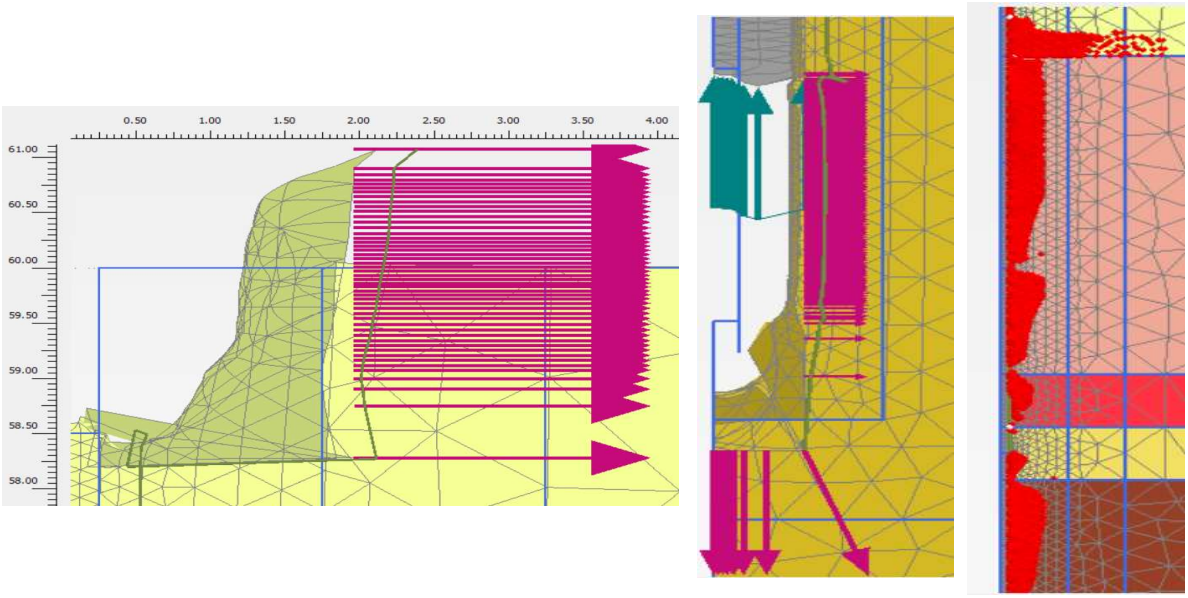

Figure 36- Soils' deformation (scaled up 50 times) and the plastification of nodes associated to the contruction/ displacement process.

4.3.3 Results and Analysis

Shaft Resistance

Following the same approach used to evaluate the shaft resistance of bored pile, on the table 11 it is presented the shaft resistance for the driven pile.

The full analysis on the shaft resistance will be done on the following sub-chapters.

Table 11- Shaft resistance of Driven Pile.

Z (m)	ZG	σ / σ' (kPa)	σmed (kPa)	ϕ (º)	δ (º)	c_u (kPa)	K_0	q_s (kN/m)	R (kN)	Total (kN)
0 3	1	0 57	28,5	30	0,367	-	0,5	5,5	26,3	2822,1
3 15	2	57 237	147	-	-	40	-	40	768	
15 17	3	237 267	252	-	-	75	-	75	240	
17 19	4	130 150	140	32	0,395	-	0,470	27,4	87,7	
19 24	5	307 397	352	-	-	120	-	120	960	
24 31,8	6	214,84 311,64	263,24	36	0,451	-	0,412	52,6	740	

It is also relevant to state that the value of K_0 reflect only the state of soil before any displacement applied. In order to optimize the theoretical value for the pile's shaft resistance it is recommended to adjust the value of it according to the value obtained by the numerical pile. This value underestimates the capacity of the shaft resistance of the pile.

Base Resistance

As the same way the bored pile model was analysed, it is also important to analyse the base capacity for the driven pile and try to understand which theory can relate better to the pile's numerical response.

Table 12- Estimated Driven Pile's toe resistance.

Base Resistance						
Theory		**N_q**	**σ0**	**q_b (kPa)**	**A_b (m2)**	**R_b (kN)**
Terzaghi		19	581,8	10803	0,16	1728
Meyerhof	m=1	370		215277		34444
	m=0	38		21964		3514
Jambu	η = 70º	23		13226		2116
	η = 90º	38		21964		3514
	η = 105º	55		32132		5141
Berezantzev	αL	**Ak**	**Bk**	10389		1662
	0,74	105	185			

The values estimated to the driven pile baring capacity are low when compared to the pile's shaft resistance. In this pile is interesting to see that the pile shaft takes an important role on the pile's capacity. When comparing the value for the estimated shaft resistance to the bearing capacity of

Terzaghi, Meyerhof (m = 0) Jambu (η = 105º) and Berezantzev, the shaft resistance can be 35 to 60% of the total resistance.

Table 13- Base resistance of the numerical Model of the Driven Pile.

Phase	Displacment Associated (mm)	Applyed Force (kN)	Force on Pile's Base (kN)	Nq associated
24	6,00	1127,8	1142,9	12,3
25	7,87	1470,9	1212,7	13,0
26	9,80	1814,0	1217,1	13,1
27	11,90	2177,8	1207,6	13,0
30	21,00	3683,8	1162,4	12,5
44	66,54	7933,4	1669,4	17,9

To better estimate the pile's ultimate capacity, it is possible to analyse the Figure 37, where the numerical model was run until it reaches its total resistance. Note that of the referred value for the bearing capacity of the pile, the Berezantzev's theory gives the better estimate to the slip surface of the soil.

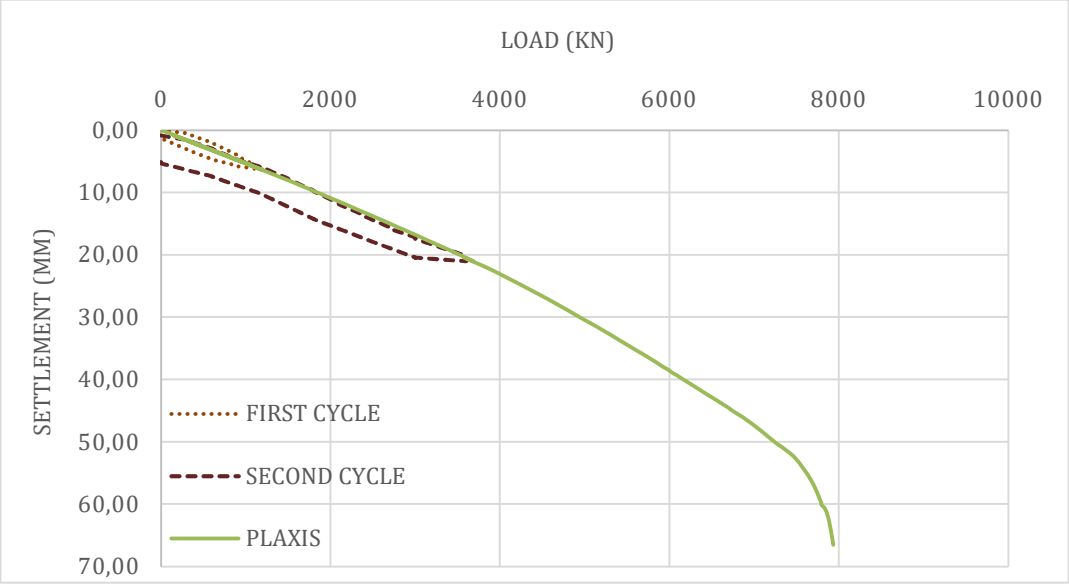

Figure 37- Rupture of driven pile for a prescribed displacement of 66,5 mm.

On figure 38 it is possible to observe the development of the plasticisation of the points on the pile's toe which indicates that the theory gives a good approximation to the model.

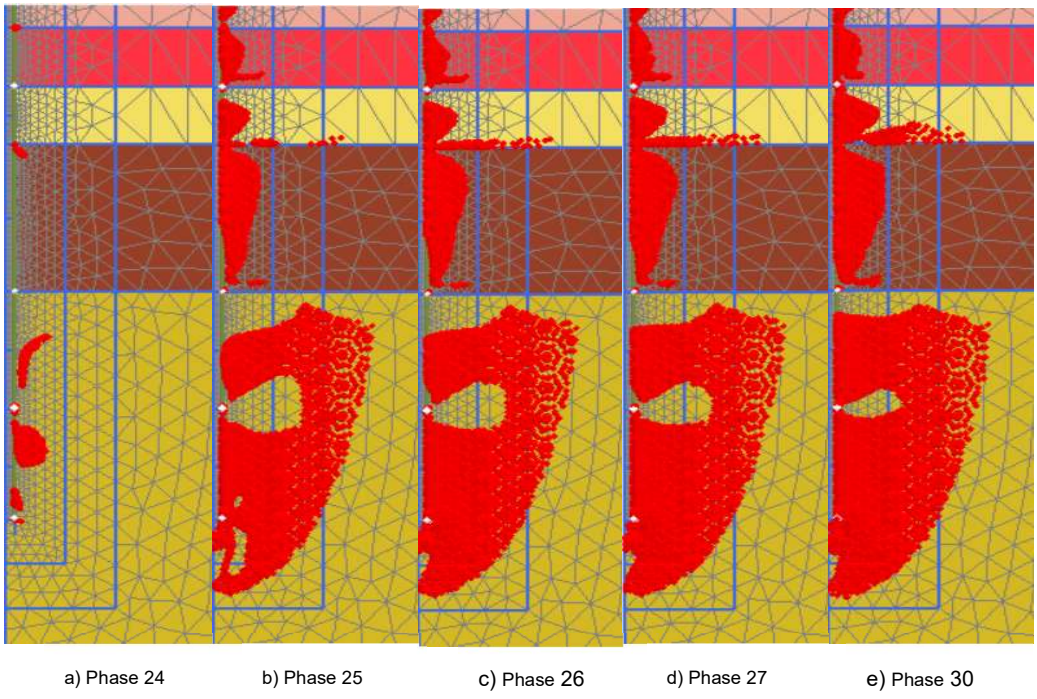

Figure 38- Plastic Bases formation during the Driven Pile Test

Wen observing the decomposition of the load in the loads carried by the base and the pile base (Figure 39), it may seem that both theories (Table 11) overestimate the results obtained by the pile. The negative force value on the driven pile shaft present on the numerical graph, once again, might be correlated to the construction process. Some authors have referred the existence of a residual load associated, more commonly, to driven piles.

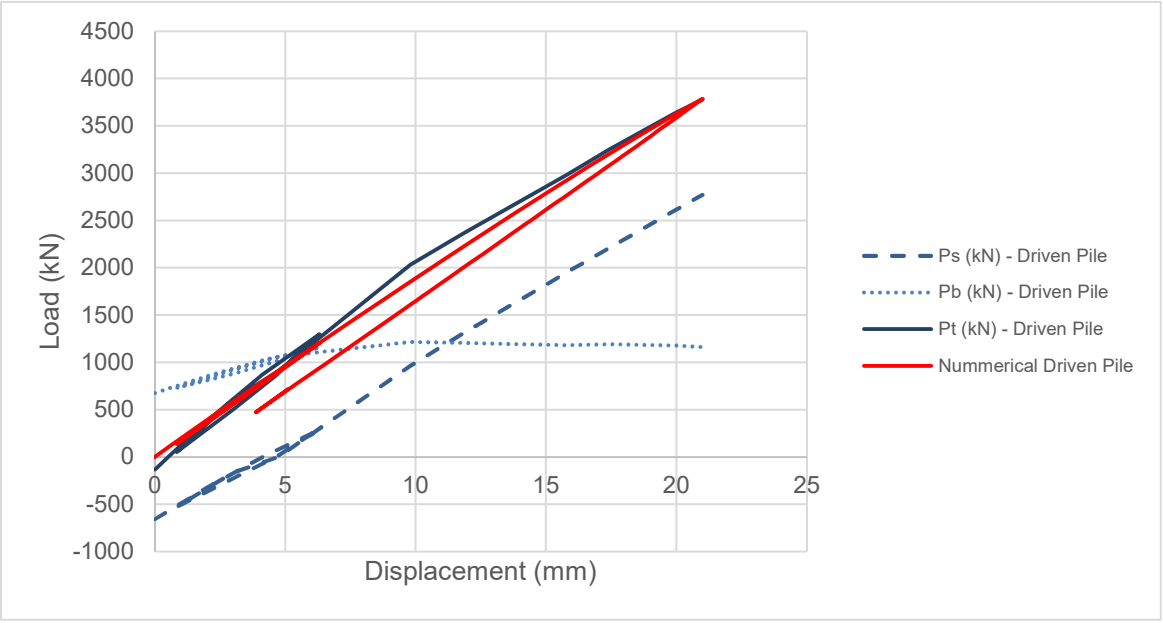

Figure 39- Decomposition of the total load on the driven pile.

Fellenius (2015) describes that during the last impact of hammer on the insertion of a driven pile into the ground it appears to be created a residual force on the pile base and along the pile is shaft. This imprisoned load is accentuated due to the consolidation that happens on adjacent soil after the pile's insertion.

The unloading makes the pile react by moving upwards and, to counter that tendency for the pile to move, the pile mobilizes some of its shaft resistance on its lower body that will, creating a negative skin friction. Additionally, the small consolidation of the soil that may exists on the pile's surroundings, tends to create a load on the upper body of the pile, but this time, in contrary direction, crating positive shaft friction.

As the Figure 37 indicates and as Figure 40 proves, the Plaxis model replicated that effect, with stresses appearing on the pile's base, creating a negative friction on the pile shaft, and the down drag effects are also present on the pile's upper body, although with a low value of positive shaft resistance mobilized when compared to the other.

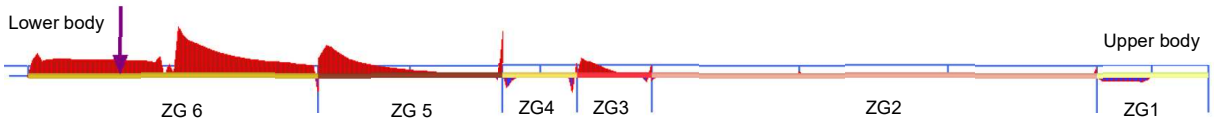

Figure 40- Mobilization of the driven pile's shaft after the installation.

The figure 41 presents a schematic presentation which behaviour was expected for the pile to have and how forces are supposed to be oriented before the loading test.

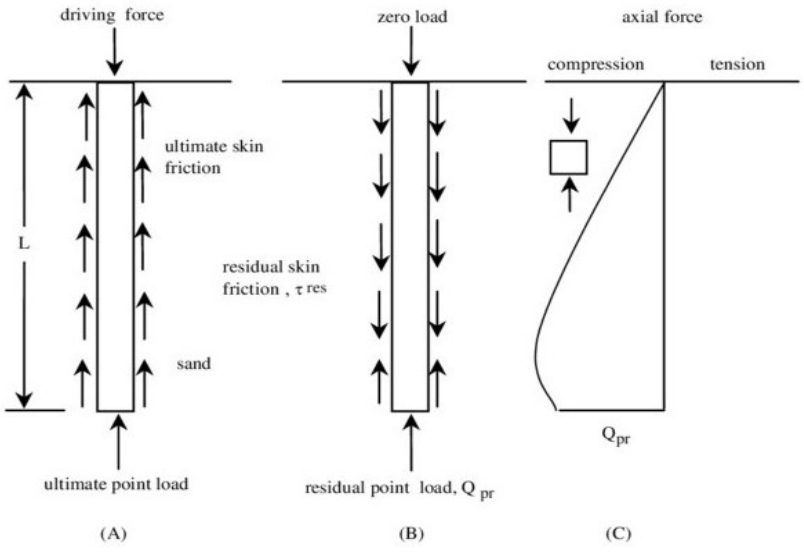

Figure 41- Residual Load on Driven Piles (Adopted from Alawneh, et al. (2001)).

Fellenius (2015) also describes that, due to this effect, the pile's response to the static load test may be misunderstood. The pile's shaft capacity has proven to be overestimated, and that it might be less that what was obtained furthermore, the pile base capacity may have been underestimated. And so, here one explanation to the low value obtain for the pile's toe capacity of driving pile.

4.4 Overall Remarks

The analysis of the behaviour of pile tests should be individually, but also comparing one pile to the other. It is important to understand if the result is according to what was expect before start and if it matches to what was enunciated on chapter 1.

The first remark that it is important to stand, from graphic on figure 42 analysis, is the enormous difference between the slopes corresponding to both displacement and bored piles. Something that would be expectable since the bored pile has twice the driven pile dimensions.

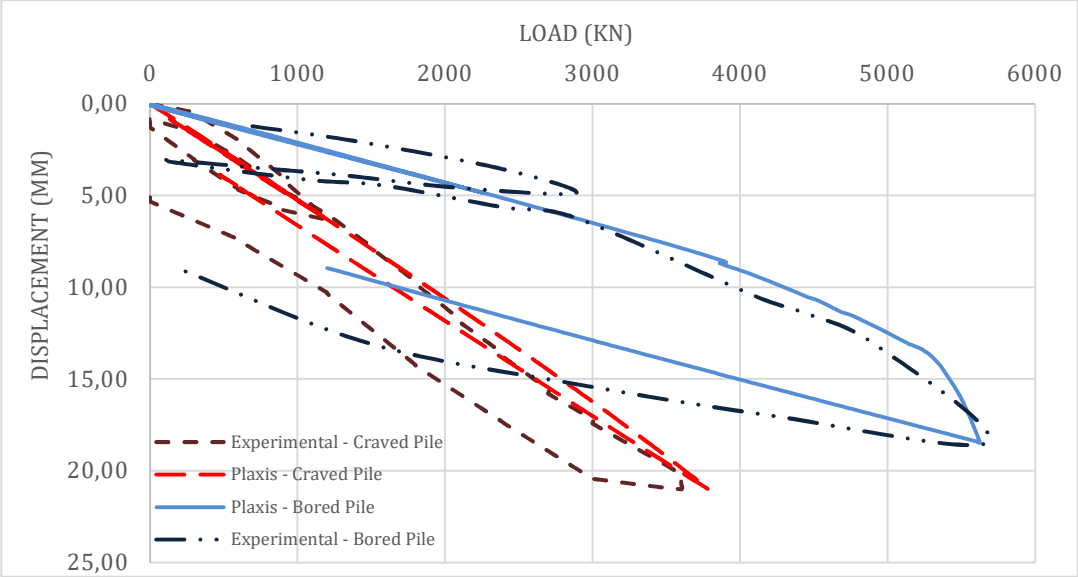

Figure 42- Load - Displacemnt curves.

To a better knowledge, it should be compared both piles capacities by unit area and see which one appears to be the more efficient solution.

Table 14- Shaft load mobilization.

	Shaft Mobilization			
	Total (kN)		Unitary (kN / m2)	
	Bored	Driven	Bored	Driven
Theoretical	4500	2822	52,7	56,5
Numerical	4436	2771	51,9	56,5
Experimental	4500	3000	52,7	60,1

The same way it was stated on the first chapter we can see a higher mobilization of force on the driven pile's shaft. The theoretical values show a lower difference once their shaft resistance is calculated the same way for both cases without taking into account the effect of the construction process of each one, the difference stands only for their lengths and the role it takes to calculate the average value of vertical stresses on the last layer of soil.

The difference gets bigger on the numerical and experimental models. This time, these two experiments consider the construction process, and as the table shows, the differences between the theoretical value with the others are higher for the displacement pile. This may induce that those formulas are more accurate to piles that do not disturb the soil at the same level as a displacement pile does.

Meanwhile, neither the numerical model nor the theoretical resistance gets the amount on the experimental shaft resistance mobilized. In fact, as it was explained, the theoretical method depreciates the construction process of the pile. It is important to account that the construction process of a driven pile has the same effect than one dynamic load test. The same way the hammer performs the dynamic test, here, the hammer hits on the pile to put it inside the soil. The numerical approach does not get close to the experimental values. Once again, as well as it was analysed before, the numerical model slightly diverges from the experimental model, also on is shaft resistance mobilized.

When observing the toe Load-Displacement curve of the bored pile of the numerical model (Figure 26) the curve development is not according to what is expected. The construction method for the excavation *i.e.*, the process of removing the soil by the bucket is not 100 per cent clean, far from that, and it has some major importance in the behaviour of the pile toe under the initial phase of loading. The bottom of the hole, during this, is mixed and is left with no significant resistance, no (or with a residual) cohesion and its elastic properties are completely distorted.

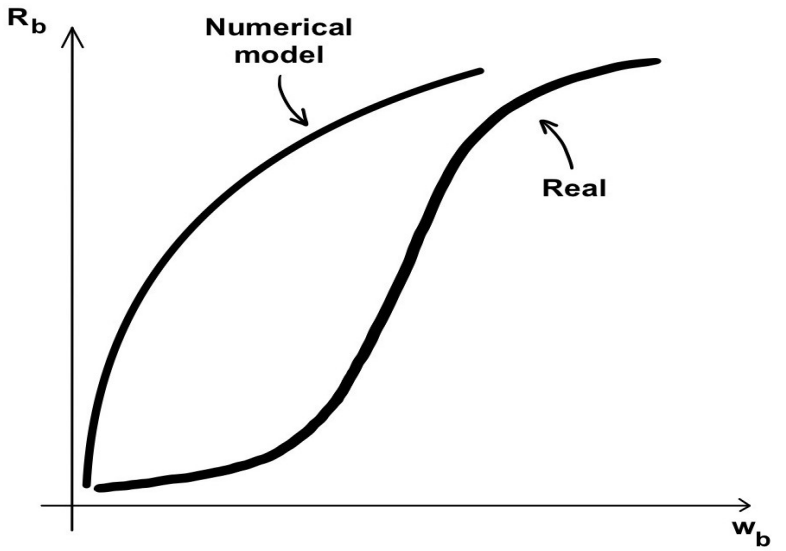

Figure 43- Load on pile's toe and pile displacement relation.

Accounting that, the curve that fits the real behaviour of the pile's toe (figure 43) should considerer the effects mentioned above. And so, the real curve of the Plaxis model should have developed an initial displacement under the first and lower stages of load. This, because the first stages of loading will only compress that softer layer and the pile will only start mobilizing its total resistance once that small zone under the pile's toe is compacted. Note also that the figure 41 is only representative and that the "Real" curve represents a heavily mixed soil on the borehole bottom.

The Figure 41 replicates this issue, where the real curve develops some displacement under low stresses on the pile's toe, then, right after the zone under pile toes gets stiffer, the displacement of the pile still occurs but this time at a lower rate than before. At his moment, the pile mobilizing the full strength of the soil where it fits, and it only stops when pile's toe reaches it total resistance.

To fully overcome this issue using the numerical software Plaxis, under the pile's toe, should be created another interface with some expression on its thickness, or it should be crated a thin layer, less than 60-50 centimetres. Both methods should considerer a strong reduction on pile properties and on pile elastic properties.

5 FINAL REMARKS

This thesis was developed with the objective to analyse the behaviour of the soil in particularly challenging conditions that are the wetlands of the Tagus River, at North Platform of North Lisbon. Defining the real behaviour of any pile under axial load is always a difficult task and not the even the initial theories for the load transfer mechanism nor for the bearing capacity of the pile can full predict the behaviour of a pile. Anticipating that, it was analysed and validated the use of numerical models for both bored and driven piles so it could provide additional information of the tests performed. Right after the characterization of the soil based on some basic tests as well as the standard penetration test and cone penetration test, it was performed a full analysis on both piles behaviour supported by the numerical information obtained by use of the software Plaxis 2D, supported by the estimated values provided by the author presented on the first chapter and, finally, by analysing the results obtained from the tests performed.

Although the results obtained were satisfactory since the numerical models estimated the shape of the experimental load-displacement curves and the theoretical methods proved to give good estimations of the bearing capacity of the pile, it is still important to refer some final notes:

On the second chapter:

- Although the equations proposed give a good estimative for both piles, they were formed based on empirical methods and so, some differences can be found from one model to another no matter how many cases proven to be right.

On the third chapter:

- Among the parameters mentioned (loading, lateral earth pressure and interface), the last one revealed to be the most significant one, with a huge role on the shaft resistance of the numerical model.
- Meanwhile, nor the dimensions of the model proposed, nor the refinement of the mesh had much influence on the results, at least for the design loads of the presented models.
- For the driven pile the amount of axial displacement prescribed on the soil under the pile's toe, during the construction process, demonstrated to have a big influence on the amount of shaft resistance carried by the pile's shaft.
- On the other side, the definition of ΣM_{stage}, does not have a big influence on the results provided by the model, since it varies very little. However, its definition is very important to prescribe the displacement without stopping the calculations of PLAXIS.

On the fourth chapter it is possible to conclude that:

- Besides the numerous data provided for the soil most simple tests (boreholes, SPT and CPTu), there exist some space for misunderstandings due the various correlations available nowadays and due to the empirical experience, that is also important for the soil classification. It is also essential that the available data provided by these testes was also limited to the analysis of charts and not the data. This leaves room for some discrepancies in the soil characterization values.
- The numerical approach and theoretical results matched well the curve load-displacement obtained from the experimental test. However, there is room to change and improve, at least in at the unloading phase, since the soil behaved as being almost total elastic.
- In the bored pile numerical analysis, the interface showed to have not such importance as it was expected, however, it depends on the model and its iterative process for the soil properties.
- The driven pile showed itself to be the most difficult test to replicate in both numerical and theoretical models. The amount of soil's displacement and plastification is still hard to quantify and so the following analysis showed to fail in some aspects. The load-displacement curve is almost perfect-elastic, what does not match the experimental results. Also, the shaft resistance of the numerical analysis showed to have not reached its limit and so, it has overestimated the results provided for both numerical and theoretical solutions.

There still exists space to improve the results and to explore more both experimental tests and the major differences between those and the theoretical approaches. The numerical analysis still has a lot to be improved so it can spot the major differences between the results obtained on field and the ones proposed by the scientific community. To latter analysis it essential to improve:

- On this work it were only explored four theories behind the bearing capacity and nowadays there a lot more that should also be considered, due to the enormous variations that a slip surface can have and how it defines the bearing capacity of a pile.
- It is relevant to have a better look at both pile's interface so it possible to better estimate the reduction on the pile's resistance properties and to estimate with a bigger effort the reduction on the elastic properties of the pile interface.
- Note also that the value of the Elastic Modulus of the pile is not constant all over the test and so it should be estimated with more certainty in many steps so that the pile test can reproduce with more accuracy the results of the test.
- The amount of displacement applied during the construction process on the numerical model should also be analysed with greater emphasis on the effects that it may have in the load-displacement pile and on the plastification of it.
- For last, the residual load showed to be essential on the interpretation of the static load test, it should be further analysed to improve the experimental result.

6 REFERENCES

A, Krasinski. Numerical simulation of screw displacement pile interaction with non-cohesive soil. Archives of Civil and Mechanical Engineering. Volume 14. Issue 1. Pages 122-133. 2014.

Alawneh, Ahmed Shlash et al. "Axial compressive capacity of driven piles in sand: a method including post-driving residual stresses". Canadian Geotechnical Journal 38. 2(2001): 364–377.

Angelino, João. Estacas de Deslocamento sob Ações Verticais. Instituto Superior Técnico. (2015). Tese de mestrado em Engenharia Civil, Instituto Superior Técnico, Universidade de Lisboa.

Ausweger, Mario & Binder, Eva & Lahayne, Olaf & Reihsner, Roland & Maier, Gerald & Peyerl, Martin & Pichler, Bernhard. Early-Age Evolution of Strength, Stiffness, and Non-Aging Creep of Concretes: Experimental Characterization and Correlation Analysis. Materials. 12. 207. 10.3390/ma12020207. (2019)

Berezantzev, V.G., and V.Alaroshenko (1962). Peculiarities of sand deformations under deep foundations. Bases, Foundations and Soil Mechanics, No. 1

Brinkgreve, R. B. (2006). Plaxis - 2D Version 8 Manual. The Netherlands: Delft University of Technology and Plaxis b. v

Bourne-Webb, P. (2019). Geotechnical Characterization. Presentation of the Special Foundations course (in Portuguese). Instituto Superior Técnico.

EN 1992-1-2, 2004. Eurocode 2: Design of Concrete Structures - Part 1-2. 1st ed. Brussels: BSi.

Fellenius, B. H. "Static tests on instrumented piles affected by residual load." DFI Journal-The Journal of the Deep Foundations Institute 9.1 (2015): 11-20.

Fleming, K. and Weltman, A. and Randolph, M. and Elson, K.. Piling Engineering, Third Edition. Taylor & Francis. (2008)Janbu, N. 1976. Static bearing capacity of friction piles. In Proceedings of the 6th European Conference on Soil Mechanics and Foundation Engineering, Vienna, Austria. Vol. 1.2, pp. 479–488.

Kulhawy, F.H. & Mayne, Paul.. Manual on Estimating Soil Properties for Foundation Design. (1990)

Liao, S.C. & Whitman, R.V. 1986. Overburden correction factors for SPT in sand. ASCE Journal of Geotechnical Engineering 112 (3):373-377.

MEYERHOF, G. G. Some recent research on the bearing capacity of foundations, Vol. 1 – n. 1 – 1963, 16-22 p.

Meyerhof, G. G. "The ultimate bearing capacity of foudations." Geotechnique 2.4 (1951): 301-332.

Mota-Engil Fundações. (2019). Memória Descritiva e Justificativa – Análise dos Reultados dos Ensaios de Carga Estática, Doc3187/DRC1/01-NT– Plataforma Logística de Lisboa Norte – Lote 19, Castanheira do Ribatejo.

Prandtl, L. (1920) “Über die Härte plastischer Körper.” Nachr. Ges. Wiss. Goettingen, Math.-Phys. Kl., pp. 74–85.

Randolph, M., & Wroth, C. (1978). Analysis of Deformation of Vertically Loaded Piles. JGED, ASCE104(GT12), pp. 1465-1488

Ribeiro, J. (2013). Behaviour of single piles under axial loading: Analysis of settlement and load distribution. Tese de mestrado em Engenharia Civil, Instituto Superior Técnico, Universidade de Lisboa.

Robertson. P.. Interpretation of cone penetration tests - A unified approach. Canadian Geotechnical Journal. 46:1337-1355. (2009).

Robertson P.K., Cabal K.L. “Guide to Cone Penetration Testing for Geotechnical Engineering”. Gregg drilling. 6th edition July 2015

Robertson, P. K., Campanella, R. G., and Wightman, A. 1982. SPT-CPT correlations. University of British Colum- bia, Civil Engineering Department, Soil Mechanics Series, No. 62, and ASCE Journal of the Geotechnical Division (accepted May 1983).

Santos, J. A. (2008). Fundações por estacas: Acções verticais. Elementos teóricos da unidade curricular de Obras Geotécnicas, Instituto Superior Técnico, Universidade de Lisboa, 25 p

Terazaghi, Karl. "Theoretical soil mechanics." John Wiley and Sons (1965).

Tjie-Liong, G. O. U. W. "Common mistakes on the application of Plaxis 2D in analyzing excavation problems." International Journal of Applied Engineering Research 9.21 (2014): 8291-8311.

7 APPENDIXS

A - Validation and comparison of the numerical model with Ribeiro (2013)

	Rint= 0,01					
	Ribeiro			Miguel		
s (mm)	Fb - Joana	Fs - Joana	Pt - Joana	Fb - Plaxis	Fs - Plaxis	Ft - Plaxis
0,00	29,23	0.42	29,66	22,65	3,66	26,31
0,10	30,07	0.49	30,56	22,92	3,67	26,59
0,20	30,88	0.54	31,42	23,18	3,68	26,86
0,30	31,68	0.60	32,28	23,46	3,69	27,14
0,40	32,44	0.65	33,09	23,72	3,70	27,42
0,50	33,18	0.71	33,89	23,99	3,71	27,70
0,60	33,90	0.76	34,66	24,25	3,72	27,97
0,70	34,61	0.81	35,42	24,52	3,73	28,24
0,80	35,31	0.86	36,17	24,79	3,74	28,53
0,90	35,97	0.92	36,89	25,05	3,75	28,80
1,00	36,62	0.98	37,6	25,32	3,76	29,08
1,50	39,58	1.26	40,84	26,65	3,81	30,46
2,00	42,21	1.55	43,76	27,99	3,81	31,80
2,50	44,58	1.80	46,38	29,32	3,81	33,14
3,00	46,71	2.05	48,76	30,65	3,81	34,46
3,50	48,67	2.30	50,97	31,96	3,81	35,78
4,00	50,45	2.54	52,98	33,25	3,81	37,06
4,50	52,10	2.73	54,83	34,48	3,81	38,30
5,00	53,68	2.86	56,54	35,71	3,81	39,52
5,50	55,45	2.90	58,35	36,85	3,82	40,67
6,00	56,79	2.92	59,71	37,52	3,82	41,34
6,10	57,11	2.92	60,02	37,34	3,82	41,16
6,20	57,43	2.91	60,34	37,35	3,82	41,17
6,30	57,67	2.90	60,58	37,37	3,82	41,19
6,40	57,99	2.89	60,88	37,39	3,82	41,21
6,50	58,27	2.89	61,15	37,40	3,82	41,22
6,60	58,55	2.88	61,42	37,42	3,82	41,24
6,70	58,80	2.87	61,68	37,44	3,82	41,26
6,80	59,07	2.87	61,94	37,45	3,82	41,27
6,90	59,33	2.86	62,19	37,48	3,82	41,29
7,00	59,59	2.86	62,45	37,52	3,82	41,33
7,10	59,91	2.85	62,75	37,55	3,82	41,37
7,20	60,12	2.84	62,97	37,59	3,82	41,41
7,50	60,91	2.82	63,73	37,69	3,82	41,51
8,00	62,20	2.79	64,98	37,86	3,82	41,68
9,00	64,44	2.75	67,19	38,23	3,82	42,04
10,00	66,80	2.70	69,5	38,59	3,82	42,40
12,00	71,01	2.63	73,64	39,25	3,81	43,07
14,00	74,97	2.56	77,53	39,76	3,81	43,57
16,00	78,70	2.49	81,19	40,06	3,81	43,87
18,00	82,18	2.45	84,62	40,34	3,82	44,16
20,00	85,46	2.40	87,86	40,64	3,81	44,45
22,00	88,59	2.35	90,94	40,97	3,81	44,78
24,00	91,61	2.30	93,91	41,26	3,81	45,07
26,00	94,48	2.25	96,73	41,48	3,81	45,29
28,00	97,26	2.20	99,47	41,48	3,81	45,28
30,00	99,98	2.16	102,14	41,71	3,81	45,52

	Rint= 1,00					
	Ribeiro			Miguel		
s	Fb - Joana	Fs - Joana	Ft - Joana	Fb - Plaxis	Fs - Plaxis	Ft - Plaxis
0,00	29,23	0,42	29,65	22,98	7,04	30,02
0,10	29,54	7,79	37,33	23,54	16,37	39,90
0,20	29,84	15,16	45,00	24,10	22,63	46,73
0,30	30,13	22,53	52,66	24,67	29,32	53,99
0,40	30,42	29,91	60,33	25,23	36,13	61,36
0,50	30,70	37,29	67,99	25,80	42,86	68,66
0,60	30,99	44,67	75,66	26,37	49,21	75,58
0,70	31,27	52,06	83,33	26,94	56,74	83,68
0,80	31,55	59,44	90,99	27,50	63,40	90,90
0,90	31,82	66,83	98,65	28,07	70,18	98,26
1,00	32,09	74,22	106,31	28,64	76,22	104,85
1,50	33,40	111,19	144,59	31,48	110,52	142,00
2,00	34,68	148,14	182,82	34,32	144,45	178,77
2,50	35,90	185,03	220,93	37,17	178,32	215,48
3,00	37,09	221,83	258,92	39,08	211,93	251,01
3,50	38,24	258,49	296,73	40,33	245,74	286,06
4,00	39,36	294,95	334,31	41,83	278,85	320,67
4,50	40,46	331,11	371,57	43,60	310,52	354,11
5,00	41,54	366,79	408,33	45,17	340,36	385,53
5,50	42,58	400,88	443,46	46,87	367,00	413,87
6,00	43,62	432,22	475,84	48,66	388,68	437,33
6,10	43,81	438,13	481,94	49,04	391,44	440,48
6,20	44,02	443,30	487,32	49,43	394,58	444,01
6,30	44,26	447,28	491,54	49,81	396,66	446,46
6,40	44,49	451,27	495,76	50,18	395,84	446,02
6,50	44,71	455,19	499,90	50,53	400,62	451,15
6,60	44,93	458,99	503,92	50,86	399,80	450,66
6,70	45,16	462,63	507,79	51,21	402,31	453,53
6,80	45,39	466,14	511,53	51,57	399,80	451,37
6,90	45,61	469,50	515,11	51,91	401,12	453,03
7,00	45,83	472,61	518,44	52,27	403,13	455,40
7,10	46,05	475,50	521,55	52,60	400,87	453,47
7,20	46,28	478,06	524,34	52,92	401,18	454,10
7,50	47,00	480,14	527,14	53,89	401,37	455,26
8,00	48,08	490,54	538,62	55,49	401,31	456,79
9,00	50,25	498,45	548,70	58,45	402,19	460,63
10,00	52,29	505,38	557,67	61,31	402,69	464,00
12,00	56,08	521,24	577,32	66,60	402,63	469,23
14,00	59,50	535,56	595,06	71,50	402,75	474,25
16,00	62,67	549,35	612,02	76,22	402,44	478,65
18,00	65,63	561,87	627,50	80,80	403,07	483,87
20,00	68,36	573,37	641,73	85,20	402,63	487,83
22,00	70,90	584,00	654,90	89,60	403,25	492,85
24,00	73,26	594,27	667,53	93,93	404,01	497,94
26,00	75,54	603,58	679,12	98,02	404,20	502,22
28,00	77,67	612,51	690,18	101,85	404,13	505,98
30,00	79,65	621,22	700,87	105,56	404,51	510,07

B – Ammount of Load Carried by the numerical models for the Case Study

Driven Pile				
phase	wt	Ps (kN) - Driven Pile	Pb (kN) - Driven Pile	Pt (kN) - Driven Pile
12	0	-657,22	676,70	-133,52
13	0,539	-566,24	724,45	5,21
14	2,024	-320,51	856,40	382,89
15	4,138	0,00	1024,79	871,79
16	6,317	289,09	1161,13	1297,22
17	5,692	192,08	1105,84	1144,92
18	4,651	0,00	1014,73	861,73
19	3,03	-223,56	882,79	506,23
20	0,838	-526,15	730,73	51,58
21	1,197	-465,84	762,78	143,94
22	2,968	-169,08	919,86	597,78
23	4,736	0,00	1061,23	908,23
26	9,802	966,98	1217,05	2031,04
27	11,9	1319,47	1207,63	2374,10
28	15,8	1954,07	1181,87	2982,94
29	17,42	2209,80	1192,55	3249,34
37	20	2616,95	1177,47	3641,42
30	21	2771,51	1162,39	3780,90

Bored Pile				
phase	wt	Ps (kN) - Bored Pile	Pb (kN) - Bored Pile	Pt (kN) - Bored Pile
2	0	118,2495	314,4734	0,722972
4	1,225	674,8141	380,4469	623,261
5	2,072	1052,434	426,0628	1046,496
6	3,556	1702,115	510,8858	1781,001
7	4,872	2275,141	610,6628	2453,804
8	4,58	2145,708	595,0176	2308,725
9	3,9	1836,575	558,3867	1962,962
10	3,533	1667,557	538,5946	1774,152
11	3,06	1451,416	513,0849	1532,501
12	0	86,89645	348,4655	3,36191
13	4,115	1940,876	570,0106	2078,887
14	4,453	2089,159	588,169	2245,328
15	5,635	2601,239	664,761	2834
16	6,213	2841,885	703,7168	3113,601
17	10,51	3699,54	1066,257	4333,796
18	11,33	3905	1110,239	4583,239
19	13,09	4284,504	1208,257	5060,761
20	18,44	4435,929	1457,071	5460,999